Isostatic rebound, active faulting, and potential geomorphic effects in the Lake Lahontan basin, Nevada and California

Kenneth D. Adams* } *Center for Neotectonic Studies* and *Department of Geological Sciences,*
Steven G. Wesnousky } *University of Nevada, Reno, Nevada 89557-0135*

Bruce G. Bills *Institute for Geophysics and Planetary Physics, Scripps Institution of Oceanography, University of California–San Diego, La Jolla, California 92093-0208*

ABSTRACT

The high shoreline of the late Pleistocene (Sehoo) lake in the Lahontan basin is used as a passive strain marker to delineate the magnitude and character of regional deformation since 13 ka. The elevations of 170 high shoreline sites document that the once horizontal (equipotential) shoreline, which traverses almost 4° of latitude and 3° of longitude, is now deflected vertically about 22 m. Most of the deformation is attributed to isostatic rebound, but a small down-to-the-north regional tilting also appears to contribute to the overall deformation pattern. Active faults locally offset the high shoreline, but cannot explain the regional upwarping attributed to isostatic rebound since 13 ka. Preliminary models of the rebound yield an upper mantle viscosity of 10^{18} Pa s that implies a Maxwell relaxation time of about 300 yr. The rapid Earth response, coupled with the rapid fall in lake level at the end of Pleistocene time, may have acted to divert some of the major rivers flowing into the basin from one terminal subbasin to another. The regional deformation caused by the rebound may also have acted to control the present location of Honey Lake. These shoreline data, therefore, support the potential for a link between climate change, deep Earth processes, and surficial processes.

INTRODUCTION

Most of the closed valleys in the Great Basin contained lakes during late Pleistocene time and during earlier periods of cooler and/or wetter climate. The increase in surface area and depth of the lakes was a direct response to climatic conditions when inflow exceeded evaporation. Although many of the closed basin lakes fluctuated only several tens of meters, a few underwent lake-level fluctuations of as much as several hundred meters (Smith and Street-Perrot, 1983). The surficial processes and depositional environments created by the lakes, and indirectly by the climate changes, had profound effects on the geomorphology of the valley bottoms where the lakes were present. Less obvious, but no less important, the filling of the lakes also affected deeper Earth processes. The substantial loads represented by the largest of these lakes caused lithospheric flexure and isostatic depression. At the end of Pleistocene time, when evaporation once again exceeded inflow, the lakes desiccated and the Earth rebounded in an equal but opposite sense. The now-deformed shorelines of these lakes offer an excellent record of the Earth's response to normal loads at relatively short wavelengths and relatively short time scales.

Lakes Bonneville and Lahontan were the two largest pluvial lakes and were located on opposite sides of the Great Basin (Fig. 1). Isostatic rebound in the Bonneville basin was first recognized by G. K. Gilbert (1890), who noted that the highest shoreline no longer prescribed a horizontal plane, but was now deflected 50 m from the horizontal. Gilbert (1890) tentatively attributed the deformation to relaxation of an elastic crust and less viscous material below after the removal of the water load. Numerous subsequent studies progressively refined the magnitude and character of rebound in the Bonneville basin and yielded estimates for the elastic thickness of the crust and rheology of the upper mantle by modeling the Earth's response (Crittenden, 1963a, 1963b, 1967; Walcott, 1970; Cathles, 1975; Passey, 1981; Nakiboglu and Lambeck, 1982, 1983; Bills and May, 1987; Bills et al., 1994). In contrast, the magnitude and character of isostatic rebound due to the substantial load imposed by Lake Lahontan on the western side of the Great Basin have received relatively little study (Mifflin and Wheat, 1971, 1979; Mifflin, 1984).

The purposes of this paper are to present evidence for the magnitude and character of deformation in the Lahontan basin since 13 ka, the time of the last (Sehoo) highstand, and to discuss potential geomorphic effects invoked by the deformation. We use elevation measurements of the high Sehoo shoreline to document deflection of this once-horizontal feature, which now varies in elevation by as much as 22 m. Although most of the deformation can probably be attributed to isostatic rebound, the contribution of post-Sehoo faulting to the overall deformation field is also assessed. Based on modeling of the deflection of the shorelines, preliminary estimates of the upper mantle viscosity below the Lahontan basin (Bills et al., 1995) and its corresponding relaxation time are used herein to assess rates of isostatic rebound and to speculate on the geomorphic effects that the rapid uplift rate may have induced.

Tectonic and Geophysical Setting of the Lahontan Basin

The Lake Lahontan basin (Fig. 2) is within an area of active tectonic deformation and historic seismicity. The former lake straddles the boundary between the Walker Lane belt (Stewart, 1988) and the Basin and Range province (Stewart, 1978) and is bounded on the east by the central Nevada seismic belt (Wallace, 1984a; Rogers et al., 1991). Ongoing deformation is expressed by abundant late Pleistocene and younger fault scarps throughout the basin (Dohrenwend et al., 1996), multiple his-

*Present address: Desert Research Institute, Reno, Nevada 89512-1095; e-mail: kadams@dri.edu.

Data Repository item 9991 contains additional material related to this article.

GSA Bulletin; December 1999; v. 111; no. 12; p. 1739–1756; 14 figures; 1 table.

toric ruptures that define the central Nevada seismic belt (Gianella and Callaghan, 1934a, 1934b; Callaghan and Gianella, 1935; Slemmons, 1957a, 1957b; Wallace, 1984b; Caskey et al., 1996), and other historic ruptures in the basin (Gianella, 1957; Sanders and Slemmons, 1979) (Fig. 3). Historic seismicity in and around the basin is primarily concentrated along the trend of the central Nevada seismic belt and along the Sierra Nevada–Great Basin boundary zone, although diffuse seismicity occurs throughout the basin (VanWormer and Ryall, 1980; Rogers et al., 1991) (Fig. 4).

The Lahontan basin is also characterized by relatively thin crust (Thompson et al., 1989) and high heat flow (Morgan and Gosnold, 1989). These geophysical estimates confirm that the basin is undergoing active lithospheric extension (Stewart, 1978; Thompson et al., 1989). Wallace (1984a) referred to most of the Lahontan basin as the "Black Rock–Carson Sink zone of extension" and inferred that the area has undergone greater and possibly more rapid extension than surrounding areas in late Tertiary time. A study by Thatcher et al. (1999) confirmed that the region occupied by Lake Lahontan is deforming more rapidly than the rest of the Great Basin. Their study shows that relatively little extension occurs across the central Great Basin but relative northwestward motion of 3.7 ± 0.8 mm/yr occurs across the central Nevada seismic belt and an additional 6.0 ± 1.6 mm/yr is accommodated across the Lahontan basin and into the stable Sierran block (Thatcher et al., 1999). This pattern of deformation appears to be broadly consistent with the seismicity of the region (Fig. 4).

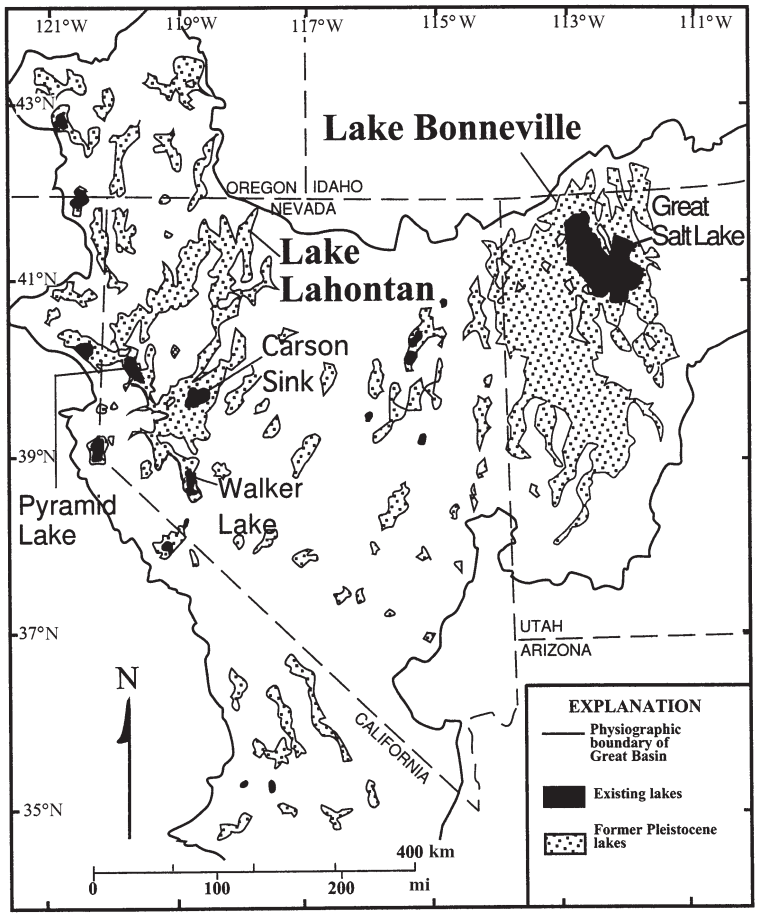

Figure 1. Location map of the Great Basin showing the locations of the larger pluvial lakes and present lakes (after Benson and Thompson, 1987b).

Deformation Measurement

Sehoo Highstand Shoreline. The Sehoo highstand lake extended through almost 4° of latitude and 3° of longitude (Fig. 2). In plan view, the lake is highly irregular and controlled, for the most part, by north-south–trending basin and range topography, except along its southwestern margin, where the lake infilled irregular structural basins formed in the Walker Lane belt (Fig. 2). The highstand lake had a surface area of about 22 500 km^2 and contained about 2130 km^3 of water (Benson and Mifflin, 1986). Water was deepest, ~270 m, in the Pyramid Lake subbasin (Benson and Mifflin, 1986). However, the largest volumes of water, and hence the greatest water loads, were concentrated in the Carson Sink and Smoke Creek–Black Rock Deserts, where water was as deep as 150 m over large areas (Fig. 2). Water was much shallower in the northeastern part of the basin because the valley floors there are higher in elevation. The general distribution of the water load can be deduced from the trace of the high shoreline. In subbasins adjacent to the Walker Lane belt and in the western half of the basin, the high shoreline is formed primarily on mountain fronts above the piedmont–range front intersection. Hence, the shoreline trace is very crenulate in detail, reflecting the corrugated nature of the range fronts. In the northeastern valleys, the trace of the high shoreline is much smoother because it is more commonly formed on the alluvial aprons being shed from the adjacent mountains (Fig. 2).

The geomorphic record inscribed by Lake Lahontan onto the mountain fronts and piedmonts in the basin is evidenced clearly by the wave-formed terraces, beach cliffs, spits, barriers, and other wave-formed features found at the elevation of the highstand and at lower levels (Fig. 5). Although there have been multiple large-scale lake-level fluctuations in the basin since mid-Quaternary time (Morrison, 1991; Reheis, 1996), the high shoreline of Lake Lahontan is an isochronous surface (Adams, 1997; Adams and Wesnousky, 1995, 1999) that probably formed in a period of years to decades immediately prior to 13 ka, the age of the Sehoo highstand (Adams and Wesnousky, 1998). This age is based on an accelerator mass spectrometry (AMS) radiocarbon date (13 070 ± 60 yr B.P.; NRSL-3014) from camel bones found in a former lagoon enclosed behind a highstand barrier. The bones were found at the contact between subaqueous lagoonal sands and primarily subaerial sediment that filled the closed depression after the lake receded from the highstand. Thus, the age of the bones closely marks the beginning of the recession of Lake Lahontan from its highstand (Adams and Wesnousky, 1998). Correlation of the high shoreline around the basin is based on detailed field studies of surficial characteristics, morphologic preservation, and soil development at multiple highstand sites (Adams and Wesnousky, 1999). Therefore, we are confident in our use of the originally horizontal (equipotential) high Sehoo shoreline as a passive displacement marker that has recorded the net deformation in the basin since latest Pleistocene time.

The high shoreline traverses a distance of

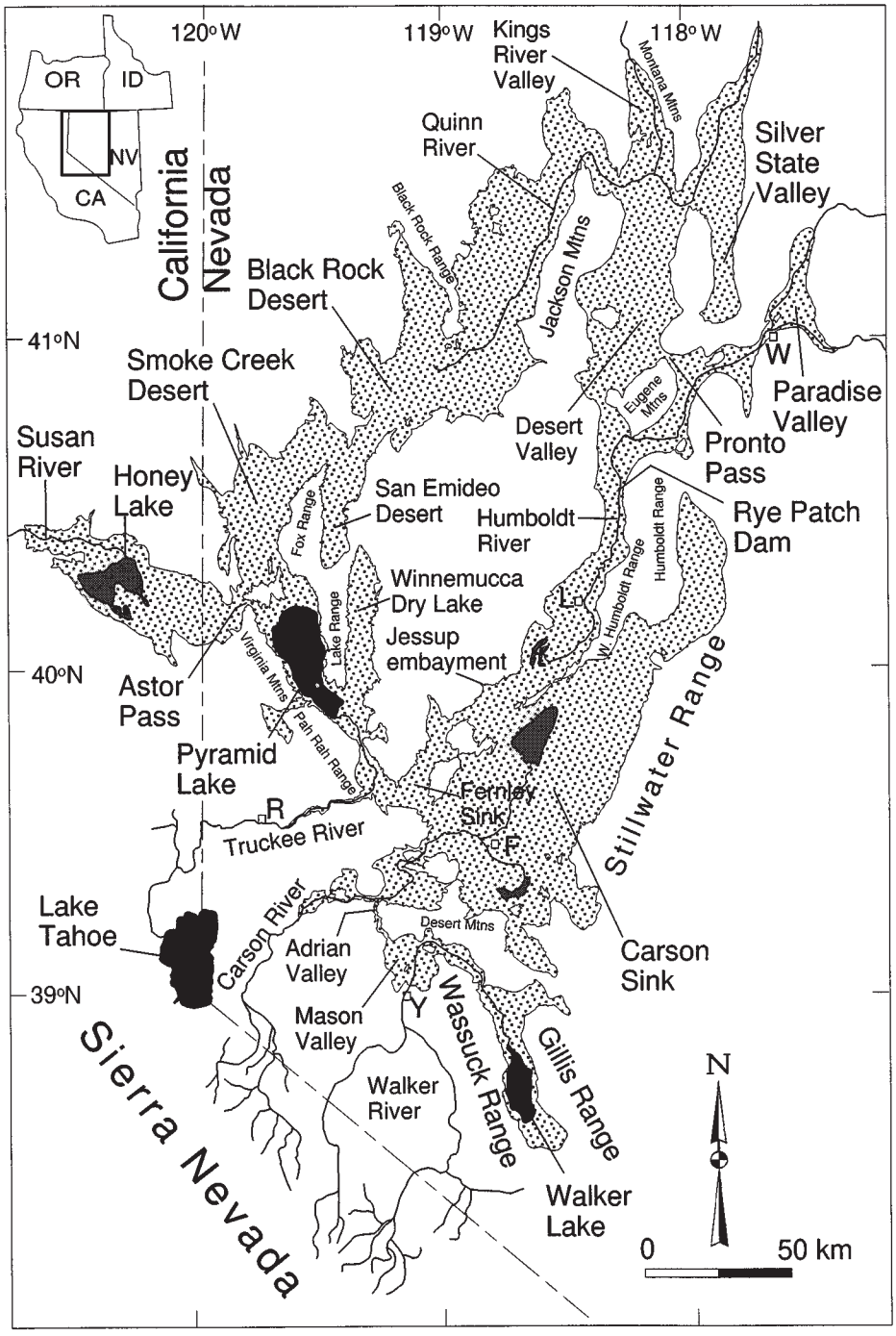

Figure 2. Map of the Lake Lahontan basin showing the locations of existing rivers and geographic features mentioned in the text. Cities: R— Reno; W—Winnemucca; L—Lovelock; F—Fallon; Y—Yerington.

~3000 km around the former islands and perimeter of the basin (Fig. 2). It is not a continuous landform, but changes character according to local conditions along its length. In some locations there are only a few rounded pebbles to mark the former highstand, but in other places well-developed shorelines are present. Wave-formed terraces are most commonly found along headlands and steep shores, and constructional features are found where there was an abundant sediment supply and local topography that permitted the accumulation of barrier forms. The degree of shoreline development was also related to the fetch and lake bathymetry. Shorelines are very strongly developed adjacent to the formerly large, deep water bodies such as the Carson Sink and Black Rock Deserts, but are very faint or absent in places where the fetch was limited or the water shallow, as in some of the far northeastern valleys (Fig. 2). Well-formed shorelines are generally well preserved but in places have been eroded by active ephemeral channels or buried by post-Sehoo alluvial fans.

Erosional and constructional shorelines found around the perimeter of Lake Lahontan were probably both the result of storm waves, but they appear to have been formed at different average heights above still water level. The elevations of shoreline angles associated with terraces adjacent to barrier ridges are always 1–3 m lower than the crests of the barriers. Detailed surveys of ten barrier crests in the Jessup embayment (Fig. 2), all within a few kilometers of one another, vary by no more than 2.6 m, suggesting that the elevation of adjacent barrier crests above their formative water plane is relatively stable. The absolute water height in the Jessup embayment at the highstand is estimated to have been about 1338.5–1339 m, which suggests that the barriers there rose from 1 to 2 m above still water level (Adams and Wesnousky, 1998). Surveys of other closely spaced shorelines around the basin also show as much as ~3 m of variation. We therefore take the natural variability in the elevations of constructional features to be about 3 m.

Methods. Potential measurement sites were selected from an aerial photographic survey of the entire Lahontan basin. All sites consist of constructional beach features that locally represent the highstand. We used constructional features because they are less prone to modification or burial after formation and they are better suited to soil correlation studies than are erosional shoreline features (Adams and Wesnousky, 1999). More than 500 potential sites were identified and located on the 17 U.S. Geological Survey (USGS) 1:100 000-scale topographic maps that cover the basin. Each site was assigned a name based on the map on which it is located. For example, potential measurement sites on the Reno sheet were numbered consecutively (e.g., R-1, R-2, R-3). If a new site was located between two existing sites (e.g., R-2 and R-3) by subsequent photo analysis or field reconnaissance, it was designated R-2a. Actual survey sites were chosen based on their distribution along the shore and their proximity to benchmarks located from USGS 1:24 000-scale topographic maps.

In the field, all sites were examined to ensure that they conformed to a basic set of selection criteria. The criteria were that the site must be the highest constructional feature located adjacent to,

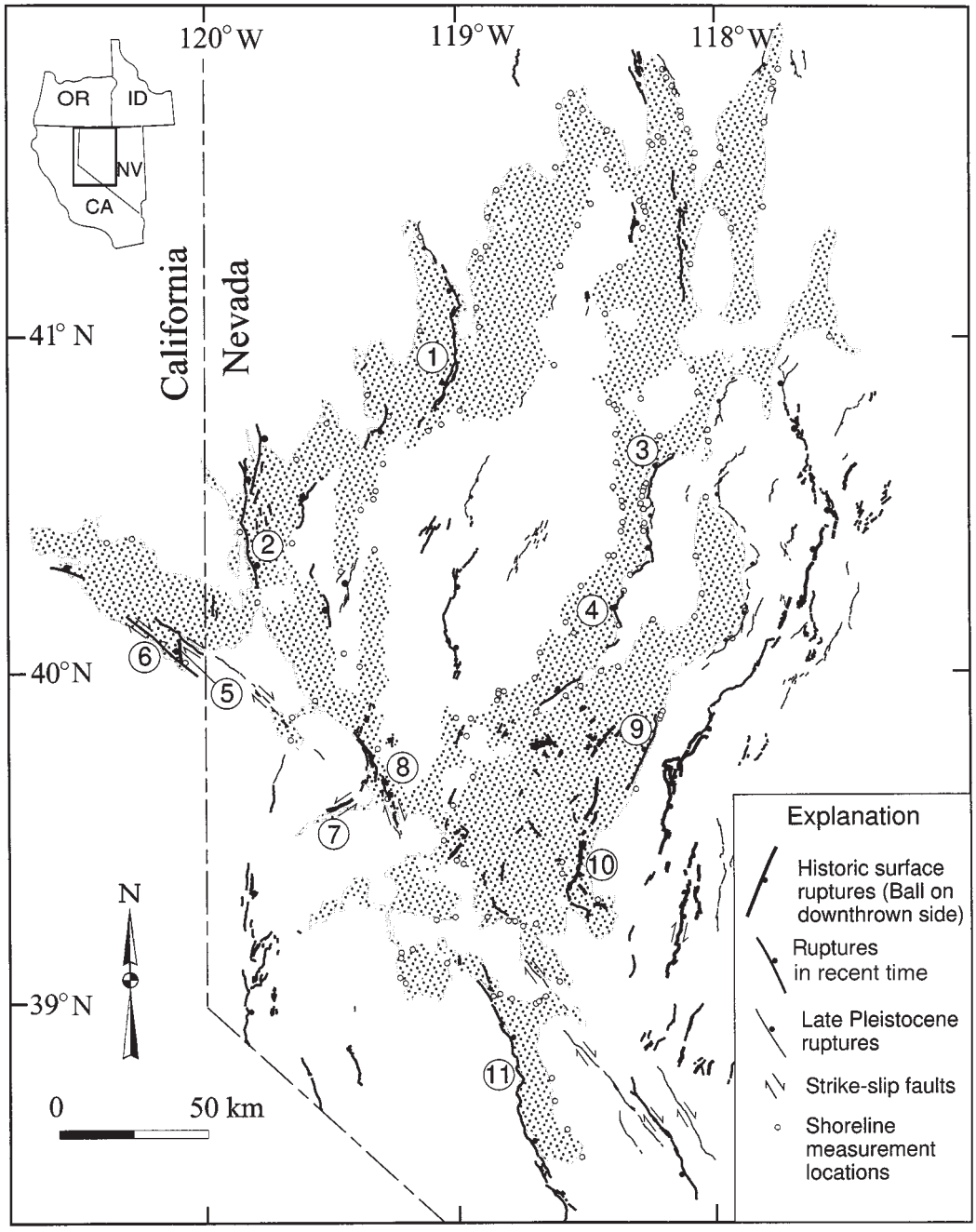

Figure 3. The distribution of young faults within and near the basin with respect to shoreline measurement sites. Numbered faults are the same as in Table 1. Fault base map is from Dohrenwend et al. (1996) and is modified by references listed in Table 1, Russell (1885), and observations made during this study.

or directly above, other lacustrine landforms. In the vast majority of cases, the crests of constructional barriers were taken to represent the highstand. When surveying the elevations of spits, where evidence of littoral drift was present, measurements were taken near their proximal ends or attachment points. No effort was made to separate swash-aligned from drift-aligned features when choosing measurement locations.

All but 3 of the 170 elevation measurements were made with a Sokkia Total Station surveying instrument referenced to local benchmarks. An attempt was made to keep distances between survey points to a minimum, but they commonly exceeded 1 or 2 km. Benchmark elevations were recorded from USGS 1:24 000-scale topographic maps according to the National Geodetic Vertical Datum of 1929. Occasionally, temporary benchmarks were established when line of site was not possible between the instrument and the shoreline or benchmark. The stated accuracy of the Total Station is ±(3 mm + 2 ppm x distance) (Sokkisha Co., LTD., 1991), yielding an error of <1 cm for a 2 km shot. However, because benchmark elevations are commonly reported to the nearest 0.1 m (or 0.1 ft), the accuracy of the measurements is assumed to be ±0.1 m.

The other three measurements (G-18, QRV-1b, and JM-12) in the data set were obtained using Trimble 4000 ST dual-frequency Global Positioning Satellite (GPS) receivers and the relative positioning technique (Dixon, 1991). In this technique we set up a base station overlying a known elevation (benchmark), while a second rover receiver was placed on the crest of a barrier, ensuring that the baseline between the instru-

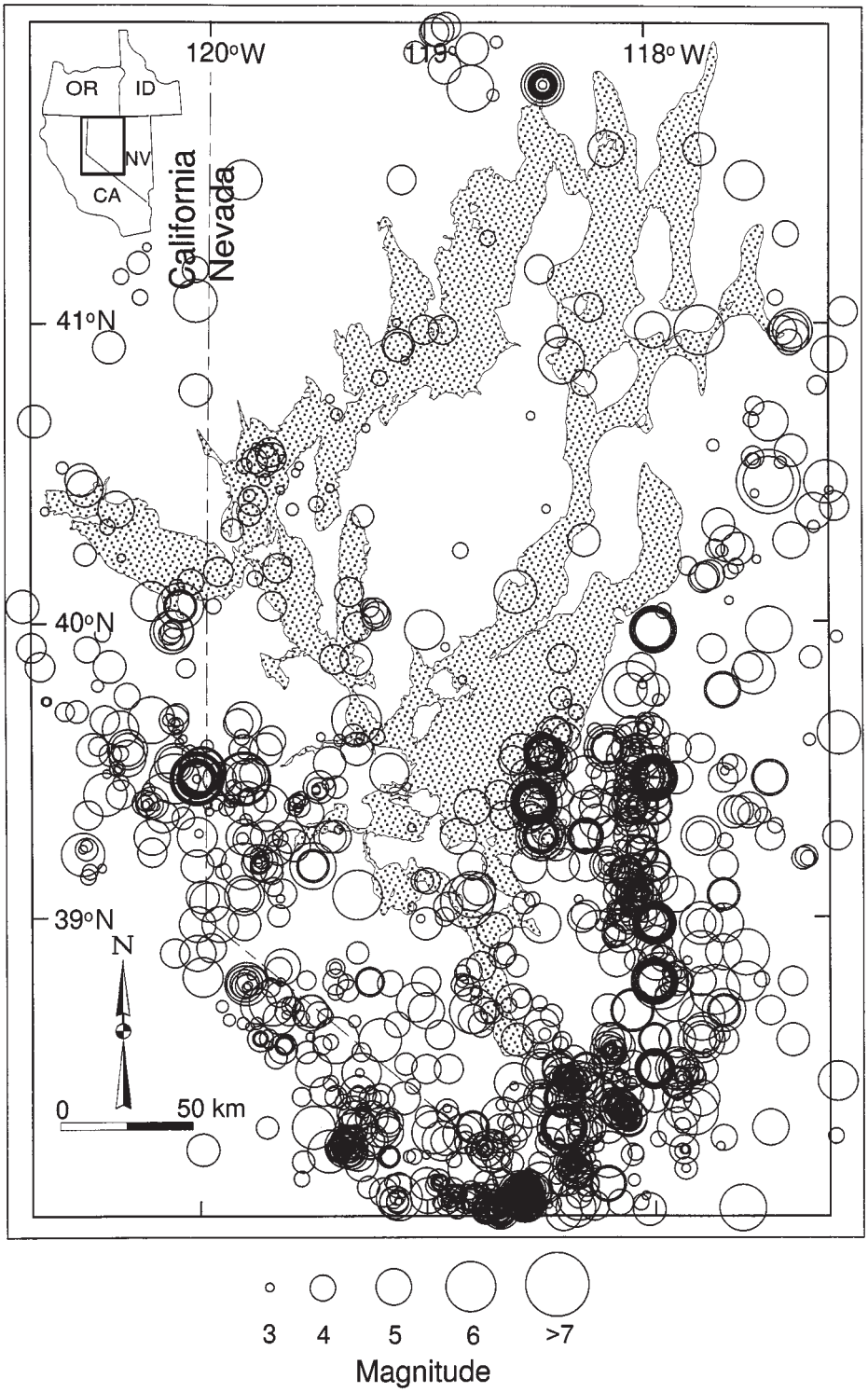

Figure 4. Historic seismicity of the Lahontan region for the period A.D. 1860–1993. Symbol sizes are graduated according to the magnitude of the earthquakes. Seismicity data are from the University of Nevada Seismological Laboratory.

ments was kept to a short distance (<5 km). Both instruments simultaneously received the broadcast signal, which was then postprocessed using TRIMVEC software to solve for the difference in elevation of the two receivers. This difference was added to or subtracted from the elevation of the benchmark. Errors associated with the GPS measurements are taken to be of the same magnitude as the errors associated with the Total Station measurements and therefore are reported to the same degree of precision. Note that the precision of both measurement techniques far exceeds the natural variability in the heights of constructional shore features (~3 m).

Results. The elevations and locations of 170 shoreline sites distributed throughout the basin are plotted in Figure 6. A table of shoreline elevations and locations is available[1]. The density of measurement locations along the high shoreline is related to the distribution of constructional shorelines coupled with the distribution of geodetic benchmarks. We examined ~250 potential sites in the field; many of these were rejected as measurement sites because they did not fit the selection criteria or we were unable to locate suitable benchmarks. High shoreline elevations range from 1318.4 m near the northern periphery of the basin to 1340.8 m near the central part of the basin. The difference of ~22 m is taken to represent the total vertical regional deformation in the basin since recession of Sehoo Lake. Shoreline elevations were hand contoured using a 3 m contour interval to characterize the magnitude and distribution of deformation (Fig. 6).

DISCUSSION

Regional Deformation

The highest Sehoo shoreline features are located in a zone extending northwestward from the northwestern Carson Sink, through the Pyramid and Winnemucca lake basins, and into the southern San Emideo Desert (Figs. 2 and 6). Lower high Sehoo shoreline features are arranged in irregular, but concentric, zones around the region of maximum uplift. The lowest high Sehoo shoreline features are located in the far northeastern valleys about 200 km north of the region of maximum uplift, where the water was relatively shallow.

The gross pattern of deformation exhibited by the high shoreline is consistent with isostatic rebound due to the removal of the Sehoo Lake load. Overall, there is a striking pattern where the

[1]GSA Data Repository item 9991, data tables, is available on the Web at http://www.geosociety.org/pubs/ftpyrs.htm. Requests may also be sent to Documents Secretary, GSA, P.O. Box 9140, Boulder, CO 80301; e-mail: editing@geosociety.org.

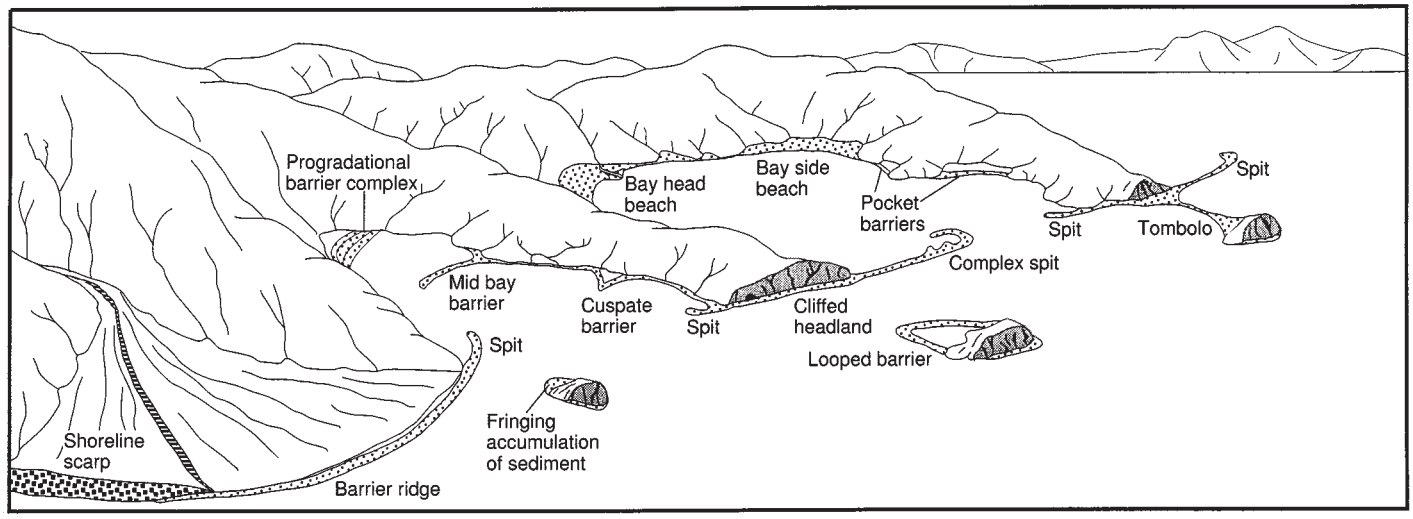

Figure 5. Shoreline classification scheme for pluvial landforms found in the Lahontan basin. Constructional shorelines accurately reflect lake level at the time of formation and are used in this study to delineate the character and magnitude of deformation within the basin (after Strahler and Strahler, 1992; King, 1972; Duffy et al., 1989).

highest elevation shorelines are located adjacent to the largest former water bodies that occupied the Carson Sink, Pyramid Lake–Winnemucca Lake, and Smoke Creek Desert–Black Rock Desert subbasins (Fig. 6). Shoreline elevations in any given area are generally similar. This suggests that the data set is internally consistent and represents regional trends. Shoreline elevations that are anomalous with respect to nearby shoreline elevations may reflect misidentification of the highstand, errors in surveying procedure, or errors in the published elevations of benchmarks. The two largest anomalies, R-3 and EM-10, are located just west of Pyramid Lake and at the southern end of the Jackson Mountains, respectively (Figs. 2 and 6). Each of these sites appears to be from 6 to 8 m too low, with respect to other shorelines in their vicinities, but neither are located adjacent to Holocene fault scarps (Fig. 3). These anomalies suggest that we may have misidentified the highstand at these locations.

North-south and northwest-southeast cross sections of high shoreline elevations across the basin document the character of lithospheric flexure (Fig. 7). Shoreline elevations used to construct the cross sections were taken from 25-km-wide bands along the lines of section. The north-south cross section (A–A′) shows a very peaked distribution centered on the Carson Sink. The northwest-southeast cross section (B–B′) also shows a peaked distribution, but is less well constrained. According to the cross-section A–A′, the high shoreline slopes to the south at about 8.5 cm/km, but slopes to the north in a more complicated manner (Fig. 7). From the center of uplift, the high shoreline slopes at about 16 cm/km for the first 50 km, shallows to about 6 cm/km for the next 140 km, but then steepens to almost 30 cm/km for the northernmost 25 km in the Kings River valley (Fig. 7). The four well-developed shorelines in northern Kings River valley are located on the hanging wall of a young fault; however, that the most recent rupture predates the highstand is indicated by truncation of the fault scarp by the high shoreline (Fig. 8). Therefore, the steep northward slope observed in Kings River valley cannot simply be attributed to faulting.

Regional northward tilting does not appear to be limited to the northernmost 25 km of the basin, but instead may involve at least the northern 150 km of the basin. In Figure 7, the lowest elevation shorelines at the south end of Walker Lake range from about 1329 to 1332 m at a distance of about 160 km from the center of uplift. However, shorelines at a distance of about 160 km north of the maximum uplift have elevations of about 1326 to 1327 m, and continue to descend to the north an additional 8 m over the next 50 km (Fig. 7).

The cause of regional down-to-the-north tilting in the Lahontan basin is difficult to resolve. We are aware of at least four processes that might contribute: collapse of the peripheral bulge associated with Canadian ice sheets, tectonic motions associated with the Yellowstone hotspot, lateral variations in viscosity structure, and complexities in the loading history of subbasins within the Lahontan system. A similar pattern of tilting is observed in the Bonneville basin (Bills and May, 1987; Bills et al., 1994). In that case, the pattern is delineated on three separate shorelines, and the rate of tilting is reasonably constant through time. In the Lahontan case, because we have only measured height variations on a single shoreline, we only know the average rate, and have no information about possible rate variations.

In both the Lahontan and Bonneville basins, collapse of the peripheral bulge created by the late Wisconsin Laurentide and Cordilleran ice sheets (Peltier, 1986) may possibly contribute to basin-wide down-to-the-north tilting. For the rate and direction of tilting in the Great Basin, from this source, to be consistent with what is observed, the elastic lithospheric thickness over most of the region between the ice margin and the lake basins needs to be close to the value assumed in Peltier's model (150–200 km). However, the local estimates of lithospheric thickness from the lacustrine rebound patterns are much less than this value (20–30 km). The influence of lateral variations in lithospheric structure on the vertical motions associated with a collapsing glacial peripheral bulge is not well understood. However, simple model calculations suggest that, if the lithospheric thickness variation occurs over a sufficiently short distance (a few hundred kilometers), there will be a locally enhanced effect at the transition.

The tectonic influence of the Yellowstone hotspot on the regions through which it has passed is spatially and temporally complex (Anders, 1994; Smith and Braile, 1994; Oppliger et al., 1997; Parsons et al., 1998; McQuarrie and Rodgers, 1998). However, it is clear that, on the southern margins of the Snake River Plain, there is a coherent pattern of tilting down toward the north over a fairly short spatial scale. It is possible that the basin-wide tilt pattern and the enhanced

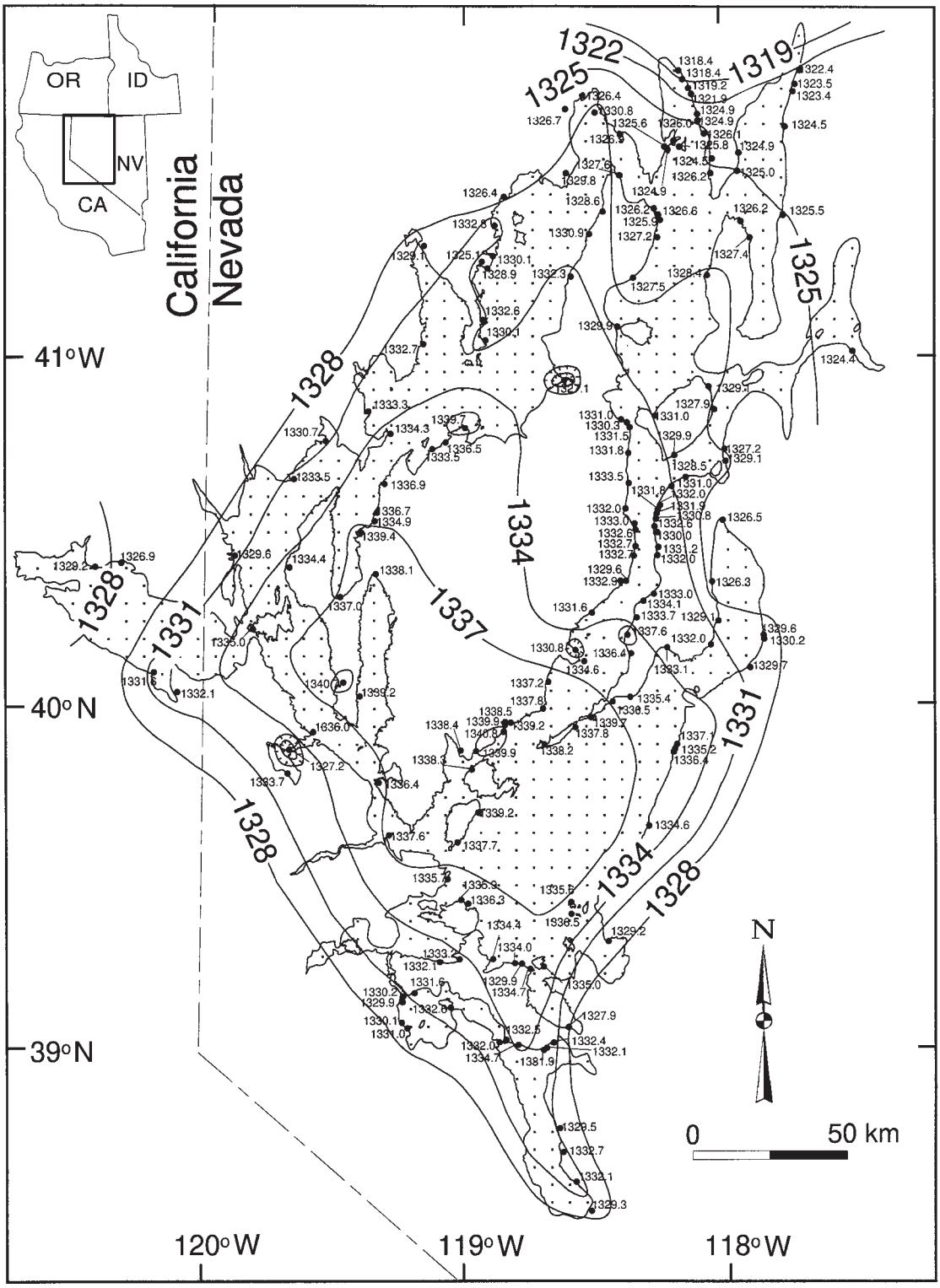

Figure 6. Map of the Lahontan basin showing the amount and character of deformation as delineated by elevation measurements of the 13 ka high shoreline. The locations of all elevation measurement sites are shown by filled circles and contoured using a 3 m contour interval. All measurements were taken on constructional beach features.

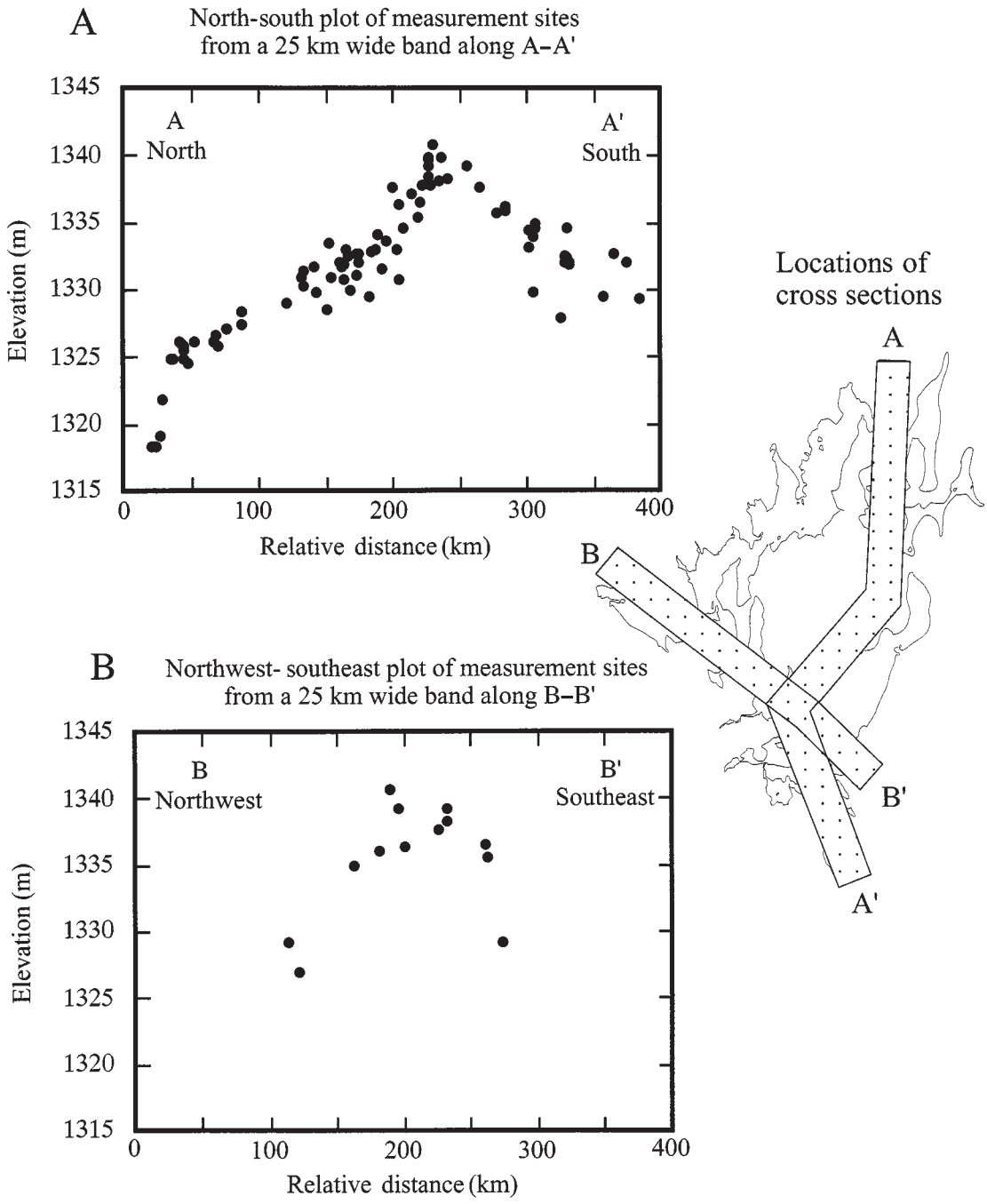

Figure 7. Cross sections of deformation in the Lahontan basin. (A) Plot of north-south cross section that displays as much as 22 m difference in the elevations of high shorelines in the basin. (B) Plot of northwest-southeast cross section that displays less, but still significant, deformation across the basin. Shorelines used to construct the cross sections are taken from 25-km-wide bands and plotted onto a single plane.

tilt seen in the northernmost shoreline observations are influenced by the hotspot effects.

The basin-wide tilting pattern is most clearly present in the difference between observed heights and those computed from the lake load and viscous flow response. The model we have used to examine the isostatic rebound process has no lateral variations in material properties, despite the fact that such variations must exist. If, for example, the viscosity were lower in the southern part of the basin, the local response to loading would be more pliant in the south. As a result, the shoreline height pattern would systematically deviate from the pattern computed using a model without lateral variations and would appear as a residual tilt.

An additional complexity in the loading process, which our current model does not properly accommodate, is the independent hydrologic histories of the Lahontan subbasins, which join together to form Lake Lahontan only at their highest

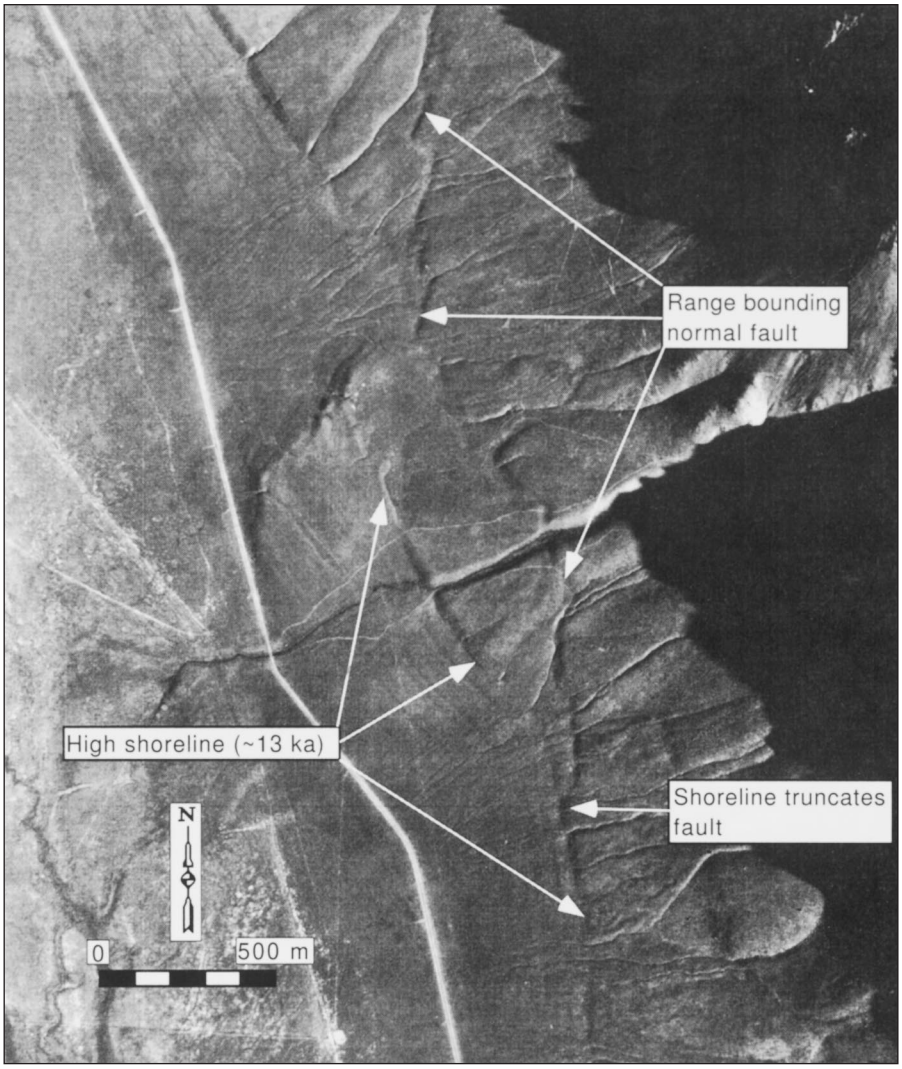

Figure 8. Vertical aerial photograph near the north end of Kings River valley. Along this section of shoreline, the Sehoo highstand is represented by both an erosional escarpment and a gravel spit. Near the south end of the photograph, the Sehoo highstand truncates a young fault scarp, demonstrating that this fault last ruptured prior to 13 ka.

levels. Because the individual subbasin hydrologic histories are not yet well resolved, we have artificially imposed a synchronous pattern of lake-level variations, even during the low-level phases when the separate lakes would actually be fluctuating independently. If, for example, the southeastern subbasins filled sooner than we have specified in our model, we will have underestimated the amount of vertical subsidence that occurred prior to formation of the measured shorelines. When lake level fell, these subbasins would rebound more than our model predicts, and an apparent down-to-the-north regional tilt would result.

Resolution of the relative contributions of these several sources of real and apparent tilt will require considerable additional work. Among the issues that need to be addressed are the loading histories of the individual basins and the patterns of rebound encoded within younger shorelines in the Lahontan basin.

The regional down-to-the-north tilting signal inferred from the Sehoo shoreline elevation data set does not appear to have acted over the long term (>100 k.y.). Coarse beach deposits of a pre-Sehoo Lake cycle, capped by a very well developed soil, are overlain by about 2 m of Sehoo highstand beach deposits at a site near the northern end of the basin in the Quinn River valley (OM-10) (Adams, 1997; Adams and Wesnousky, 1999). If regional down-to-the-north tilting had been operating through much of late Quaternary time, it is likely that the older beach deposits would not be found in close vertical proximity to the Sehoo highstand deposits at the northern end of the basin.

Shoreline and Fault Interactions

The relationships between active faults and Sehoo landforms and deposits provide a means with which to place gross limiting ages on fault activity and to assess the amount of offset on individual faults since 13 ka. However, it is more difficult to assess the effects of individual faults on the cumulative deformation of the high shoreline. The distribution of shoreline measurement sites with respect to young faults in the basin (Fig. 3) provides limited spatial resolution for determining fault deformation. The effects of small (<3 m) fault displacements on the regional deformation field are difficult to assess because the resolution in defining the elevation of the high shoreline over a broad area is limited to about 3 m. The following discussion is presented within these confines.

Young fault scarps are truncated by the high shoreline along the west side of the Montana Mountains (Fig. 8), the west side of the Jackson Mountains, and along the southeast side of Buena Vista Valley at the base of the Stillwater Range (Hanks and Wallace, 1985) (Fig. 3). These truncations demonstrate that the most recent ruptures along these faults occurred prior to 13 ka. There are many other faults in the region that have not ruptured since 13 ka, but their precise age is not known (Dohrenwend et al., 1996).

The number of faults that offset Sehoo shorelines or deposits is also large. Table 1 presents a compilation of data from selected faults in the basin that have been active since 13 ka. Other faults have also been active during this time interval, but little is known about them other than their recent activity (Fig. 3). The numbered faults in Table 1 are keyed to the numbered faults in Figure 3 and are generally arranged from north to south. The Honey Lake, Warm Springs Valley, Pyramid Lake, and Olinghouse fault zones are all located within the Walker Lane belt and predominately exhibit strike-slip displacement with little accompanying vertical displacement (Table 1 and Fig. 3).

The Wassuk Range front fault zone also is within the Walker Lane belt, but displays large Holocene dip-slip displacements. Demsey (1987) documented two post-Sehoo ruptures with cumulative displacements of 6–7 m along this zone. Displacement estimates are based on measured fault scarps and offset shore deposits, both of which represent near field deformation. Based on comparisons with the average elevations of unfaulted shorelines on the east side of Walker Lake, the absolute uplift of the Wassuk Range

TABLE 1. SELECTED YOUNG FAULTS IN THE BASIN THAT DISPLACE SEHOO LANDFORMS OR DEPOSITS

Fault name	Sense of displacement	Most recent rupture	Number of Holocene events	Cumulative recent vertical offset	
				Average	Maximum
1. Black Rock fault zone[1]	Normal	<1100 yr B.P.	2?	1–2 m	8.3
2. Bonham Ranch fault zone[2]	Right-oblique	~290 yr B.P.	2	1.5–2.5	3.5
3. Humboldt Range front fault zone[3]	Normal	<13,000 yr B.P.	1	1–2?	?
4. West Humboldt Range front fault zone[11]	normal	<13,000 yr B.P.	1	3?	3?
5. Fort Sage Mountains fault zone[4]	Normal	A.D. 1950	1	0.12	0.20
6. Honey Lake fault zone[5]	RL strike-slip	<500 yr B.P.	4	?	?
7. Olinghouse fault zone[6]	LL strike-slip	A.D. 1869	1?	?	0.9–4.3
8. Pyramid Lake fault zone[7]	RL strike-slip	<300 yr B.P.	5?	?	?
9. Western Stillwater Range front fault zone[8,11]	Normal	<13,000 yr B.P.	1	3?	3?
10. Rainbow Mountain fault zone[8,9]	Right-oblique	A.D. 1954	2?	0.3–0.5	0.8
11. Wassuk Range front fault zone[10]	Normal	<13,000 yr B.P.	2	6–7	7

Notes: Numbers of locations correspond to numbered locations in Figure 3. Sources of data: 1: Dodge (1982); 2: Weick (1990); 3: Wallace (1987); 4: Gianella (1957); 5: Wills and Borchardt (1993); 6: Sanders and Slemmons (1979), Bell (1984); 7: Anderson and Hawkins (1984); 8: Bell (1984); 9: Rodgers et al. (1991); 10: Demsey (1987); 11: this study.

due to these faulting events ranges from 0.5 to 3.0 m (Demsey, 1987).

Both the Black Rock (Dodge, 1982) and the Bonham Ranch fault zones (Weick, 1990) have also had relatively large Holocene displacements (Table 1). However, unlike the Wassuk Range front, the maximum displacements along the Black Rock and Bonham Ranch fault zones are limited to small sections of the faults; the average displacements are considerably less (Table 1). In all three fault zones, though, the distribution of shoreline measurements and the corresponding rebound contours (Fig. 6) does not allow us to confidently assess the Holocene far-field deformation associated with these faults.

Shoreline deformation along the West Humboldt Range may be attributable to post-Sehoo fault displacement. Due east of Lovelock, Nevada, the range-front fault displaces a group of barrier beaches by about 3 m (Fig. 9). The scarp profile was measured on a recessional barrier, but the displacement value probably also applies to the high shoreline because of its close proximity. Comparison of the elevation of the high barrier (1337.6 m) located on the footwall with those in close proximity suggests that this shoreline may have been elevated by about 1 m or more above surrounding shorelines by the post-Sehoo rupture. However, the difference in elevations is close to the resolution (~3 m) with which we can define the high shoreline elevation, illustrating a very important point. Almost all of the post-Sehoo vertical displacements, excluding the Wassuk Range front, reported in the literature and observed during the course of this study are less than or equal to about 3 m. Therefore, while measurement of shoreline elevations is an effective technique to delineate the character and overall regional pattern of vertical deformation in the basin, it is generally too coarse to delineate the contributions of discrete fault offsets. More detailed surveys would be required to document the uplift patterns associated with particular faults. The observations lead us to the conclusion that the overall pattern of deformation, as defined by the high shoreline, is due to isostatic rebound coupled with regional northward tilting and that the effects of localized faulting are below the resolution of our method.

Potential Geomorphic Effects of Isostatic Rebound

Deflection of the highstand shoreline reflects upper mantle flow back beneath the basin after the desiccation of Sehoo Lake. Both the magnitude of deformation and the rate at which crustal rebound occurred may have been sufficient to influence surficial processes. The magnitude of rebound at any given point in the basin can be estimated by subtracting the current elevation of the high shoreline from the prerebound elevation. In this study we assume that the elevation of 1328 m closely approximates the prerebound value of the high shoreline because symmetrical deformation across the central part of the basin seems to bottom out at about this elevation (Fig. 7). Shorelines below this elevation in the northeastern part of the basin have probably been affected by regional down-to-the-north tilting. The rate at which the rebound occurs is a function of the magnitude of rebound as well as the viscosity of the upper mantle.

Loads at the Earth's surface are supported by a combination of buoyancy and elastic strength, with viscous flow modulating the temporal response. Buoyant support is governed by Archimedes's Principal; a load emplaced on the surface of the Earth will displace an amount of matter with a mass equal to that of the load. The effect of a subsurface layer with significant elastic strength is simply to enlarge the region over which buoyant support of a load occurs. The effect of viscous flow is to mediate the transition from prompt regional elastic support to final local buoyant support.

In an elastic solid material, stress is proportional to strain. In a viscous fluid material, stress is proportional to strain rate. The elastic rigidity of crustal or upper mantle rocks can be determined from laboratory experiments or seismic wave propagation velocities, and is typically ~10^{11} Pa (Pascal = Newton/m^2 = 10^{-5} bar). Estimates of upper mantle rock viscosity values are generally in the range 10^{18}–10^{21} Pa s.

Earth materials generally exhibit a combination of elastic and viscous behaviors. The Maxwell model of viscoelastic behavior has the desired property of behaving elastically on short time

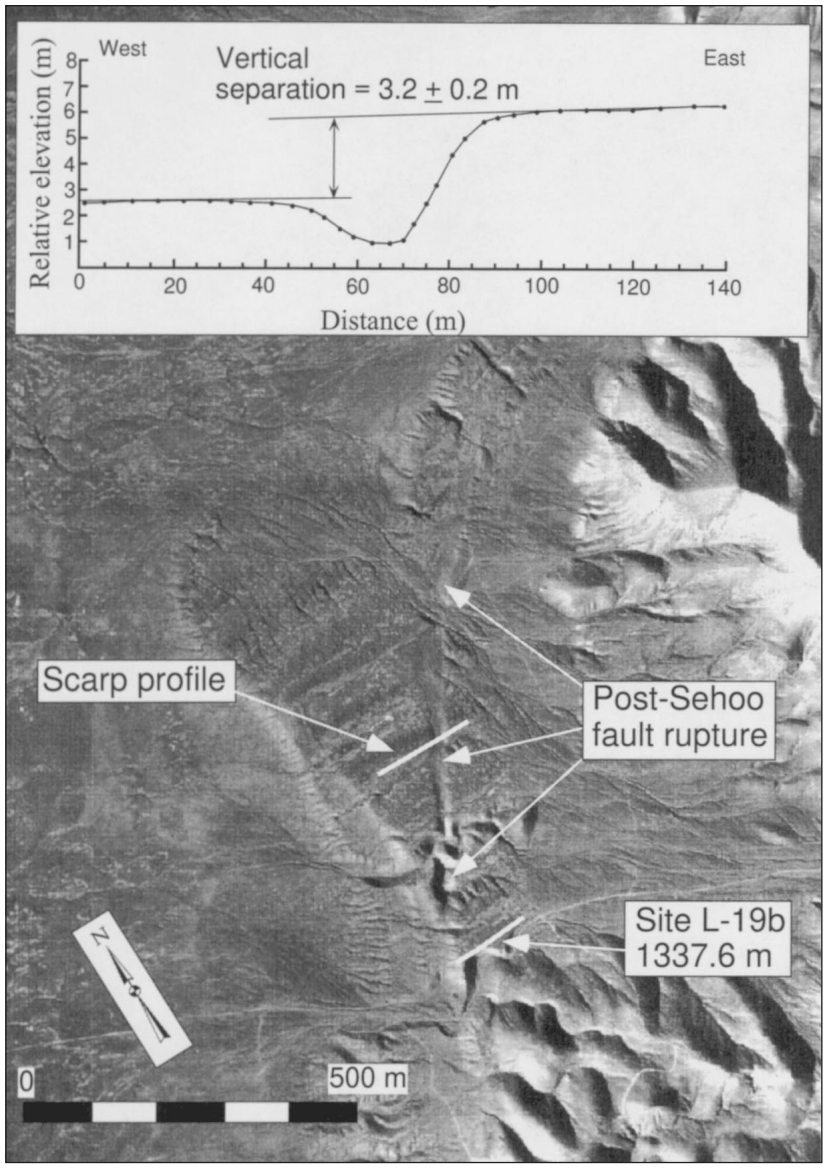

Figure 9. Vertical aerial photograph of the West Humboldt Range front near Lovelock, Nevada. A Holocene (post-Sehoo) fault offsets Sehoo shorelines by about 3.2 m (inset scarp profile), and may have superelevated the high shoreline (site L-19b) at this location. See text for discussion.

scales and viscously on long time scales. In that model, the strain rates (rather than the strains) are presumed to be additive. That is, the total strain rate is the sum of viscous plus elastic contributions. The time required for transition from prompt elastic response to ultimate buoyant response is given by the ratio of the viscosity to the rigidity, and is called the Maxwell relaxation time.

A preliminary estimate for the viscosity of the upper mantle beneath the Lahontan basin is on the order of 10^{18} Pa s, which suggests a Maxwell relaxation time of about 300 yr (Bills et al., 1995). Following a hypothetical instantaneous removal of the water load, the deformation pattern will decay away with relaxation times that are somewhat wave-length dependent, but are all equal to or longer than the Maxwell time. Thus, roughly 50% of the deformation is recovered in the first 200 yr, 50% of the remaining deformation is recovered in the next 200 yr, and so forth. The viscosity estimate is based on the modeling approach outlined in Bills et al. (1994). The approach entails four basic steps: specification of an input spatio-temporal load signal (lake-level history), specification of a density and depth-stratified Earth model, calculation of the vertical displacement field corresponding to the times and locations of measurement sites, and comparison of the observed deflection to the modeled deflections. The low value of viscosity for the upper mantle suggests that the rebound rate in the Lahontan basin was rapid, probably on the order of 1 cm to several centimeters per year during the years and decades following the rapid decline in lake level from the highstand.

Lake Lahontan began to recede from its highstand by 13 070 ± 60 yr B.P. (Adams and Wesnousky, 1998) and had reached an elevation of 1230 m in the Winnemucca Dry Lake subbasin by 12 070 ± 210 yr B.P. (Thompson et al., 1986), implying an initial desiccation rate of at least 11 m/100 yr. Although rapid, the rate of desiccation was probably not a limiting factor on the rate of rebound but allowed uplift to proceed at much higher rates than occur due to present-day tectonic stresses.

The upper mantle viscosity estimates calculated from the Lahontan shorelines are considerably lower than typical global average viscosity estimates obtained from glacial isostatic models. A plausible explanation for that difference is that the upper mantle beneath the Great Basin is hotter than the global average. That interpretation is well supported by observations of high heat flow (Lachenbruch, 1978), recent volcanism, and extensional tectonics (McKee and Noble, 1986; Minster and Jordan, 1987; Zoback, 1989). For a recent review of the geophysical structure of this region, see Humphreys and Dueker (1994a, 1994b).

The rapid uplift in the basin, coincident with the rapid desiccation of the lake, may have contributed to the diversion of some of the major rivers into different terminal basins. As lake level declined, rivers entering the basin were progressively lengthened across the former lake bed. The initial character of the newly exposed lake bed was probably relatively flat because, as the lake filled at the beginning of the Sehoo period, deltaic and lacustrine sediments likely back-filled preexisting river trenches. Dissection observed along the Truckee, Carson, Walker, and Humboldt Rivers most likely occurred during Holocene time as the rivers were adjusting to an entirely new set of climatic, hydrologic, and base-level controls. The gradients of all rivers flowing into the basin progressively decreased through time as the basin continued to uplift. The effect of lessening gradients on the rivers, coupled with other factors such as fluctuating water and sediment discharge, may have caused the rivers to change their courses away from areas of greatest localized uplift.

The Humboldt, Walker, and Truckee Rivers (Fig. 2) are unusual because, at times in the past, each flowed into a different terminal basin than where they now end. Evidence for river diver-

sions in the Lahontan basin includes the existence of paleochannels (Russell, 1885; Jones, 1933; King, 1978, 1993; Davis, 1982, 1990), probable distribution of former deltas (Davis, 1987), the isotopic composition of former lake waters (Benson and Peterman, 1995), and inferences based on the interpretation of lake bottom cores (Benson and Thompson, 1987a; Bradbury et al., 1989).

The Walker River currently flows north through Mason Valley, then makes an abrupt turn to the south to flow into Walker Lake (Figs. 2 and 10). At various times in the past, however, the Walker River continued north through Adrian Valley and joined the Carson River as a tributary to flow into the Carson Sink. The idea that the Walker River once flowed through Adrian Valley was first proposed by Russell (1885), who deduced that the valley must have been excavated prior to the deposition of the upper lacustral clays (Sehoo-equivalent deposits). King (1978, 1993) presented the salient physical evidence that the Walker River at times flowed through Adrian Valley. Both Benson and Thompson (1987a) and Bradbury et al. (1989) presented evidence from cores within and tufa dates from around Walker Lake suggesting that the lake was a playa ca. 15 ka, which strongly supports the view that the Walker River was flowing into the Carson Sink at that time. At some point just before the Sehoo highstand, Walker Lake became integrated with the rest of Lake Lahontan, probably through a sudden flooding event produced by spill as Lake Lahontan backed up into northern Mason Valley (Morrison and Davis, 1984). After Lake Lahontan fell from its highstand, Walker Lake became a playa until ca. 4800 yr B.P. (Benson and Thompson, 1987a; Bradbury et al., 1989), when it had relatively high lake levels until ca. 2700 yr B.P. High lake levels, separated by periods of shallow lakes, also occurred at 1250 yr B.P. and within the past 300 yr (Benson et al., 1991). Although some of these fluctuations may be attributed to regional climate fluctuations (Bradbury et al., 1989; Stine, 1994), others were probably due to diversion of the Walker River into and away from Walker Lake (Benson and Thompson, 1987a; Benson et al., 1991).

The behavior of the Walker River since the recession of Sehoo Lake may have resulted from the interactions between rebound and fluctuations in sediment and water discharge. Multiple active and inactive channels associated with the Walker River slope gently to the north across the relatively nonincised sediment-filled trough of Mason Valley (Fig. 10). King (1993) first delineated a paleochannel that diverges from the present path of the Walker River in the vicinity of Yerington, Nevada, and passes into Adrian Valley to become a tributary of the Carson River. The morphological characteristics of the paleochannel are very similar to those of the modern Walker River channel. Long profiles of the two channels are also very similar and are separated at their point of diversion by a vertical distance of <3 m (King, 1993). After desiccation of Lake Lahontan, the river continued to flow into the Carson Sink until about 4800 yr B.P., when it changed course and began to flow into Walker Lake (Benson and Thompson, 1987a; Bradbury et al., 1989). The local rebound contours (Figs. 6 and 10) suggest that the river maintained its drainage to the Carson Sink until mid-Holocene time, because a river channel trending northwest through Mason Valley is parallel to contours of post-Sehoo uplift. The gradient of a river flowing northeast through Mason Valley would progressively decrease as rebound proceeded, causing preferential river migration to the west. During mid-Holocene time, increased sedimentation in the paleochannel, possibly accompanied by periods of drought (Davis, 1982), may have caused the river to avulse to the east where it would then flow into Walker Lake. Because the paleochannel and modern channel now have essentially identical long profiles, subsequent avulsion events in late Holocene time may explain the switching of the river course from Walker Lake to the Carson Sink and back again. However, additional work on the past and present channels of the Walker River is needed to confirm its behavior in post-Sehoo time.

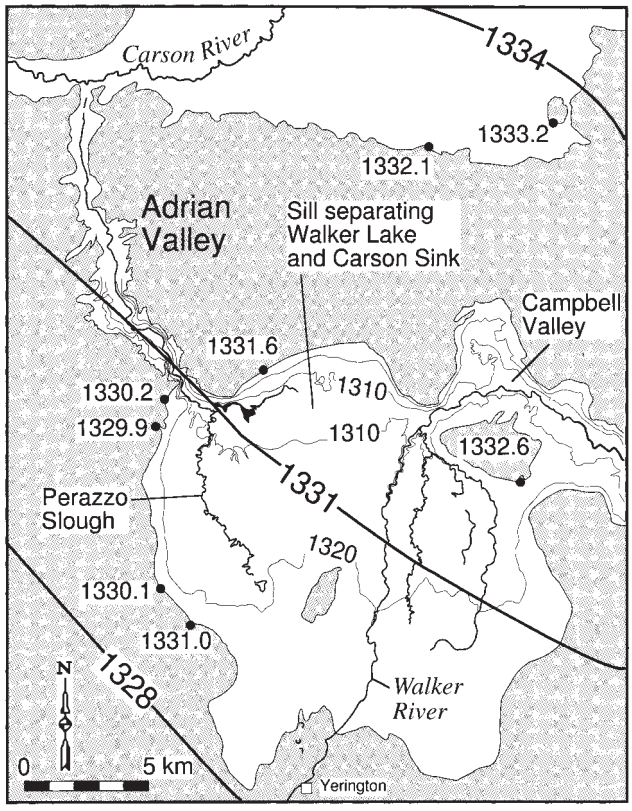

Figure 10. Map of the Mason Valley area showing the locations of the present channel of the Walker River, the postulated paleochannel (Perazzo Slough), topographic contours, and local rebound contours. High shoreline measurement sites are designated by filled circles. The former extent of Lake Lahontan is designated by the unshaded area. All elevations are in meters.

The Humboldt River also has a history of switching into different subbasins. During filling of Sehoo Lake, the Humboldt flowed through Pronto Pass and into Desert Valley, which is part of the Black Rock subbasin (Figs. 2 and 11) (Davis, 1982, 1990; Benson and Peterman, 1995). As Sehoo Lake receded, the Humboldt River entrenched a canyon through a broad alluvial divide in the vicinity of Rye Patch Dam and now terminates in the Humboldt Sink (Fig. 11). From stratigraphic studies in the vicinity of Rye Patch Reservoir, Davis (1987, 1990) found that the canyon south of Rye Patch Dam was newly cut at the end of Pleistocene time and the youngest previous channel through the divide is 600–700 ka. Therefore, the Humboldt River must have been discharging through Pronto Pass and into southern Desert Valley through much of the period since early Pleistocene time. This inter-

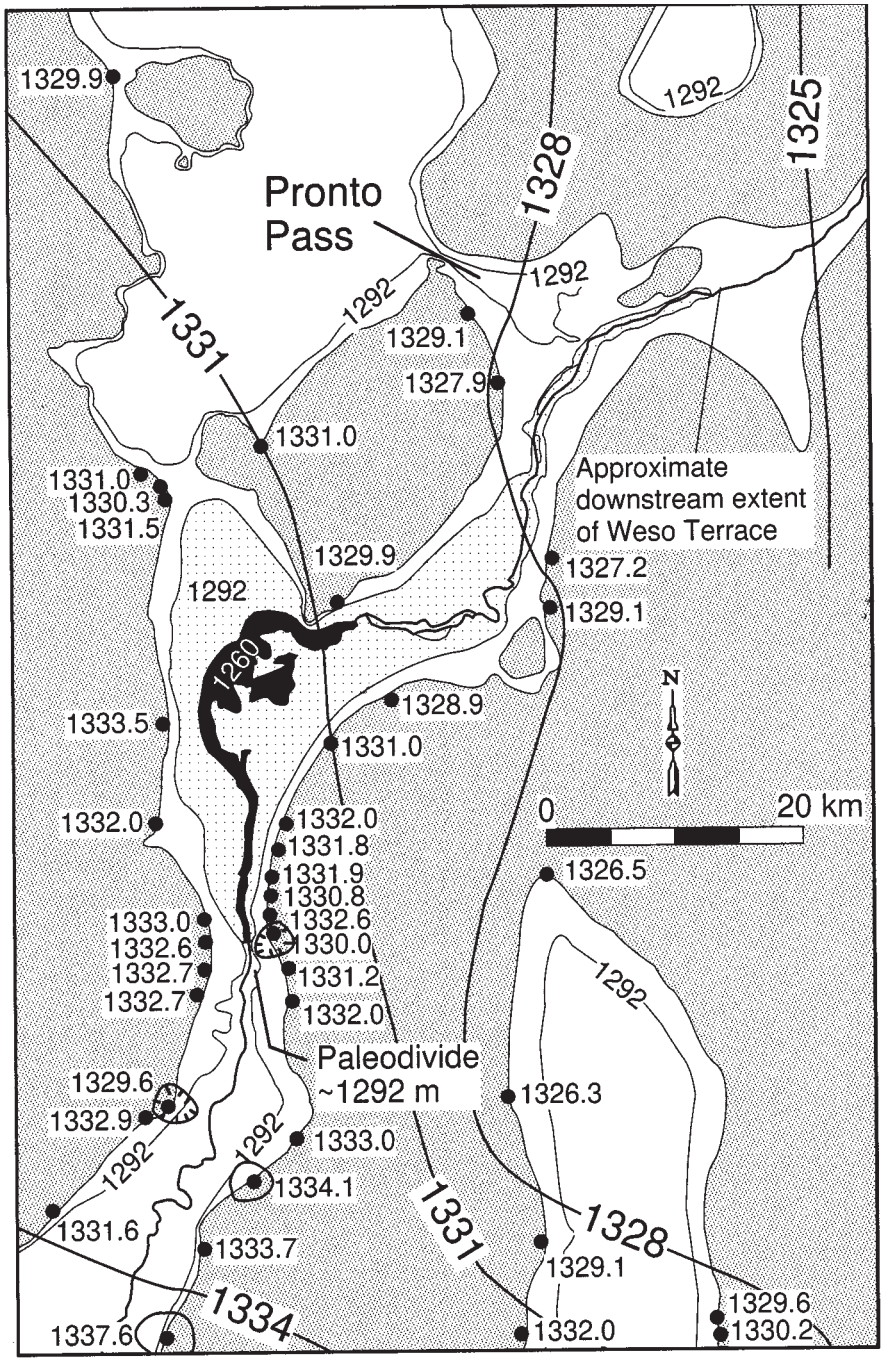

Figure 11. Map of the Humboldt River valley in the vicinity of Rye Patch Reservoir that portrays the relevant features related to the diversion of the Humboldt River. Both Pronto Pass and the reconstructed paleodivide near Rye Patch Reservoir are near an elevation of 1292 m. If the Humboldt River was diverted toward Rye Patch after the Sehoo Lake cycle, a substantial lake (stippled area below 1292 m) would have ponded behind the paleodivide. The present canyon at Rye Patch was likely cut when the ponded water overtopped the paleodivide. The former extent of Lake Lahontan is designated by the unshaded area. High shoreline elevations are designated by filled circles, and rebound contours are shown by thick black lines. All elevations are in meters.

pretation is supported by the anomalous concentration of sand sheets and dunes originating from a postulated paleodelta in southern Desert Valley and trending east-northeast through southern Silver State and Paradise Valleys north of Winnemucca (Fig. 2) (Davis, 1987). Isotopic evidence for the Humboldt River flowing into the Black Rock system during Sehoo time was presented by Benson and Peterman (1995). They determined that rivers draining the Sierra Nevada have much lower $\delta^{87}Sr$ values than the Humboldt River and used this information to demonstrate that the $\delta^{87}Sr$ values of tufas deposited in the Pyramid Lake subbasin prior to 15 ka were influenced by Humboldt River water entering the subbasin via the Desert Valley–Black Rock system.

Davis (1990) proposed that the diversion of the Humboldt River at the end of Sehoo time occurred because the broad alluvial divide around Rye Patch Dam was isostatically depressed relative to the area around Pronto Pass (Fig. 11). However, our rebound data show that, at most, there was about 3–4 m difference in the potential rebound at each location, with shorelines in the Rye Patch Dam area only slightly higher (Fig. 11). The broad flat area immediately east of Pronto Pass is covered by Holocene sand dunes that display an irregular topography with an average elevation of about 1290 m. The local rebound contours are oriented north-south near Pronto Pass, indicating that as rebound progressed during and after the Sehoo desiccation, the gradient of a river flowing west through Pronto Pass would be reduced (Fig. 11). A reduced westward gradient may have increased sedimentation in this area, and both effects may have acted to divert the Humboldt River to the south, parallel to the local rebound contours. If this occurred, a substantial lake would have ponded behind the broad alluvial divide located downstream near Rye Patch Dam. The elevation of the divide is about 1292 m, which is nearly identical to the elevation of Pronto Pass and to a shoreline mapped on the east side of Rye Patch Reservoir by Davis (1983). We infer that the ponded water topped the Rye Patch divide first and that rapid downcutting formed the present canyon. The giant incised meanders along the Humboldt River south of Rye Patch Dam (Davis, 1990) are possibly a result of this rapid discharge event. Fluvial terraces upstream of Rye Patch Dam may lend support to this sequence of events.

Hawley and Wilson (1965) described the Weso terrace, which is the oldest post-Sehoo fluvial terrace in the Winnemucca area, and inferred that it is graded to the elevation of the former alluvial divide near Rye Patch Dam. Weso terrace remnants are well preserved and extensive above Winnemucca, but are only found downstream to a point roughly coincident with the 1292 m topographic contour, located east of Pronto Pass (Fig.

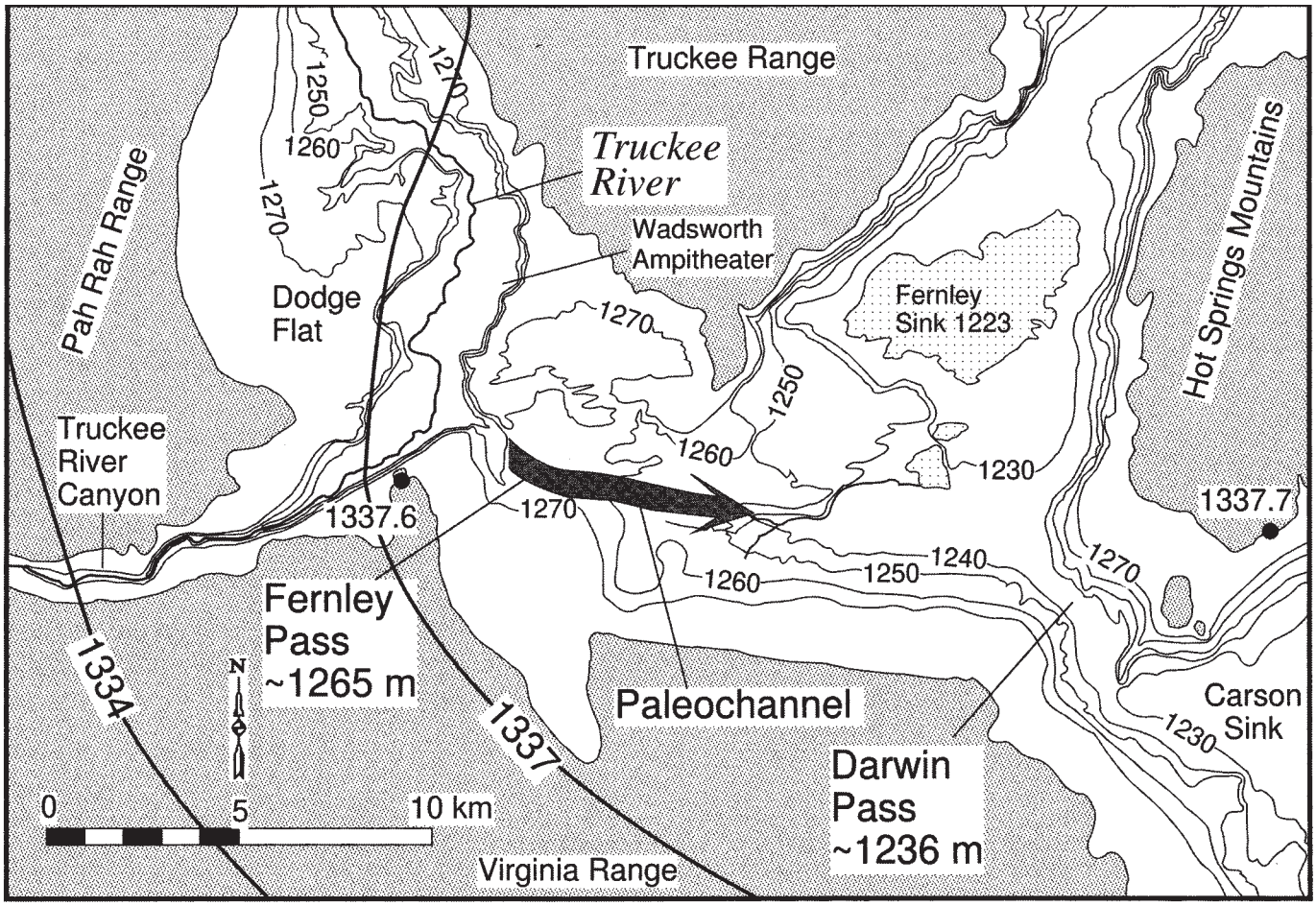

Figure 12. Map of the Fernley Pass area showing the present path of the Truckee River and the hypothesized paleochannel that may have been briefly occupied during the recession of the Sehoo Lake. The broad areas around Fernley Pass and Dodge Flat, at an elevation of about 1260–1270 m, probably represent the surface of a paleodelta of the Truckee River. The former extent of Lake Lahontan is designated by the unshaded area, and the Fernley Sink playa is shown by a light stippled pattern. Topographic contours from 1230 to 1270 m are shown by thin gray lines, rebound contours are shown by thick black lines, and high shoreline elevations are shown by filled circles. All elevations are in meters.

11). This terrace has a lower gradient than younger fluvial terraces and the modern channel in the same area (0.52 m/km vs. 0.66 m/km) and is characterized in places by a relict braided-stream pattern (Hawley and Wilson, 1965), suggesting a high sediment discharge at the time of its deposition. We tentatively suggest that the deposits of the Weso terrace aggraded in response to the rising lake ponded behind the alluvial divide near Rye Patch Dam and that the present gradient of the terrace may have been affected by isostatic rebound, but confirmation of these hypotheses must await further work, including surveying and dating of Weso terrace sediments and shorelines in the Rye Patch Reservoir area.

The Truckee is another example of a river that may have been diverted to a different subbasin because of the effects of isostatic rebound. As the Truckee River exits its deeply incised bedrock canyon between the Pah Rah and Virginia Ranges, it takes an abrupt 90° turn to the northwest and terminates at Pyramid Lake (Fig. 12). In the vicinity of Fernley, Nevada, the river is incised about 30 m into a package of surficial deposits that include the outcrops of the Wadsworth Amphitheater (Russell, 1885; Antevs, 1925; Morrison, 1991; Morrison et al., 1965; Morrison and Davis, 1984; Smoot, 1993). Much of the incision may have occurred in post-Sehoo time, which indicates that upon Sehoo Lake recession the Truckee River was lowered onto a relatively flat surface at about 1265–1270 m (postrebound elevation). What appears to be an abandoned river channel continues east from the vicinity of Fernley into the Fernley Sink. Jones (1933) first noted this channel, but interpreted it to be pre-Lahontan in age. During the initial lowering of the Truckee River onto this surface the river may have occupied this channel, but because local rebound contours are oriented northwest-southeast (Figs. 6 and 12), the sense of uplift would have the effect of lessening its gradient. Continued rebound may have had the effect of diverting the river to the northwest, parallel to rebound contours, where it became incised into its present channel as base level continued to lower.

The location and existence of Honey Lake may also be at least partially controlled by the effects of isostatic rebound. Honey Lake is located in the west-central part of Honey Lake Valley and is fed primarily by water from the Susan River. The lake covers a large area, about 200 km^2, when the lake surface is at about 1215 m, but is rather shallow (~3 m) and has repeatedly desiccated in historic time (Rockwell, 1990). Holocene ruptures of both the Honey Lake fault zone and the Warm Springs Valley fault zone trend into the lake (Fig. 3) (Grose et al., 1990; Wills and

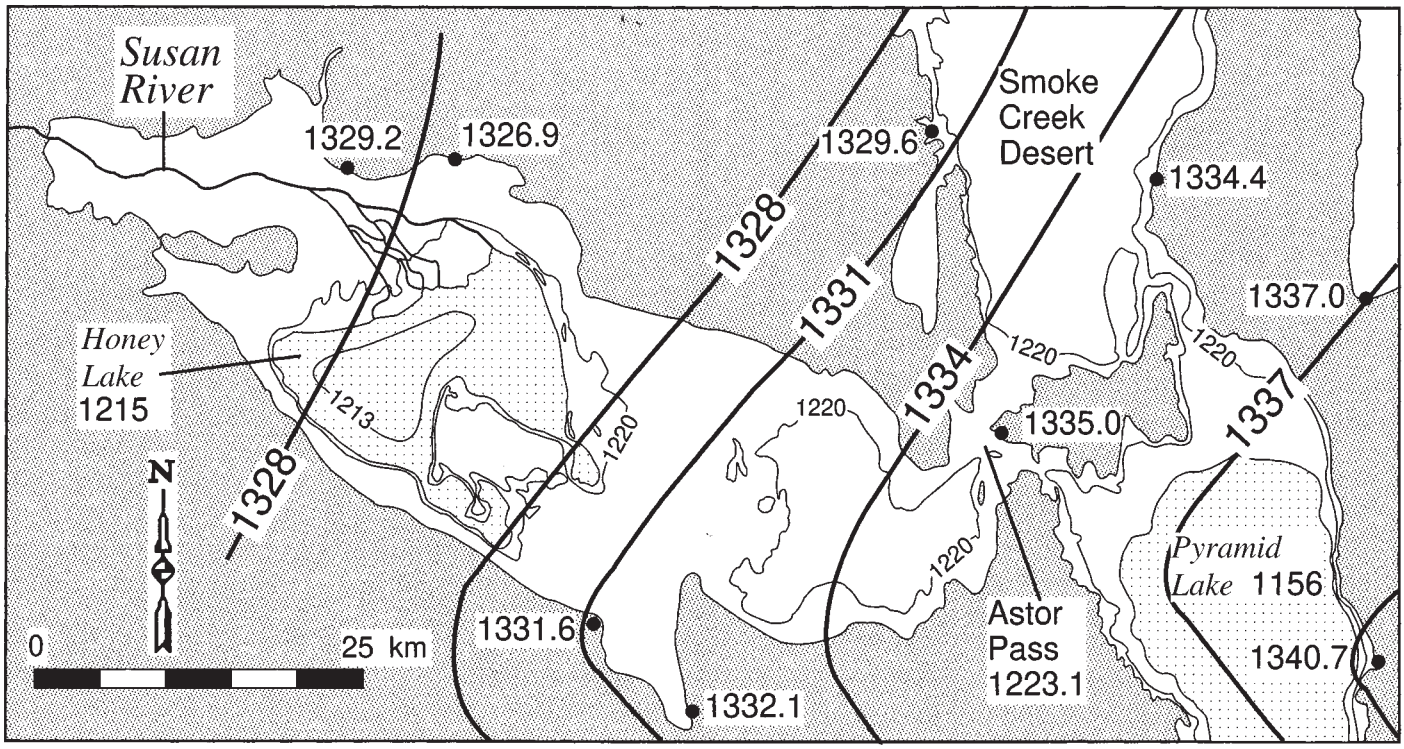

Figure 13. Honey Lake Valley showing the present location of Honey Lake and other geographic features in the area. The former extent of Lake Lahontan is designated by the unshaded area, and Pyramid and Honey lakes are shown by a light stippled pattern. The 1220 m topographic contour is designated by a thin gray line, and rebound contours are designated by thick black lines. High shoreline elevations are designated by filled circles. All elevations are in meters.

Borchardt, 1993). The interaction between these two right-lateral strike-slip systems may have had the effect of locally down-dropping part of the area occupied by Honey Lake, but this seems counterintuitive because the lake is in a left stepover between these two systems. On a larger scale, the lake is located at the foot of a broad shoulder of rebound that rises to the southeast (Figs. 6 and 13). The current floor of Honey Lake Valley is relatively flat and horizontal, but by subtracting the magnitude of rebound from the assumed prerebound elevation (~1328 m), an east-sloping gradient would be restored to the eastern half of Honey Lake Valley (Fig. 14). This would either cause the Susan River to have flowed through Astor Pass and directly into Pyramid Lake, or at least to have localized Honey Lake in eastern Honey Lake Valley. It seems plausible that Honey Lake may have slid into its present position in response to regional effects of isostatic rebound, but confirmation must await further detailed study.

CONCLUSIONS

Elevation measurements on the late Pleistocene high shoreline of Lake Lahontan define the character and magnitude of regional deformation in the basin since 13 ka. The total vertical deformation on this once horizontal (equipotential) surface is about 22 m. The resolution to which the signal can be measured is limited to about 3 m because of natural variability in the height that constructional beach features form above a still water plane. Because the zone of maximum uplift is coincident with the largest former water loads, we attribute most of the deformation to simple isostatic rebound. A secondary regional down-to-the-north tilting is also apparent and may be related to one or more of the following: (1) collapse of the peripheral bulge associated with Canadian ice sheets; (2) tectonic motions associated with the Yellowstone hotspot; (3) lateral variations in viscosity structure; and (4) complexities in the loading history of subbasins within the Lahontan system. The down-to-the-north tilting does not appear to be a long-lived phenomenon because pre-Sehoo shore deposits are exposed directly below Sehoo highstand deposits in the northern part of the basin. Within the resolution of our technique, local post-Sehoo faulting does not appear to modulate the overall vertical deformation pattern.

Even though the fact that rivers have been diverted from one subbasin to another has been fairly well established (Russell, 1885; Jones, 1925; King, 1978, 1993; Davis, 1982, 1990; Morrison and Davis, 1984; Benson and Peterman, 1995), the cause of these diversions has been poorly understood. We propose that rapid isostatic rebound during and after the rapid desiccation of Sehoo Lake, due to an anomalously low viscosity upper mantle beneath the basin, may in part be the cause of these diversions. In each case, the rivers appear to be deflected away from the local rebound gradient. The lessening of already low river gradients, in combination with fluctuating sediment and water discharge rates, may explain the diversions toward different subbasins.

The subbasin into which the newly diverted river flows gains much in terms of wetlands or lakes and corresponding habitat, while the subbasin that loses the river dries up and becomes relatively barren. If isostatic rebound has played a role in these diversions, or in controlling the location of Honey Lake as we have also proposed, then this phenomenon points to a process link between climate change (creating and desiccating lakes), upper mantle flow, and large-scale geomorphic and paleoenvironmental effects.

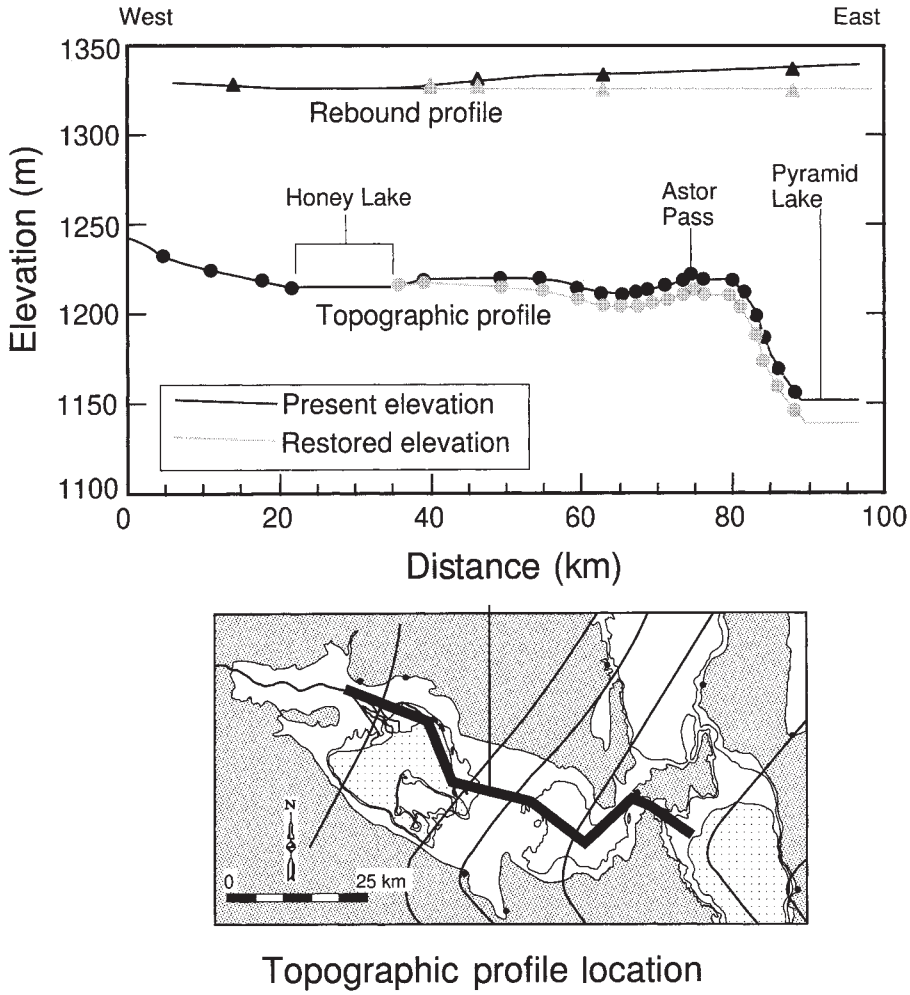

Figure 14. Profiles of deformation and topography in Honey Lake Valley. If uplift due to isostatic rebound is restored back to the horizontal, and the same correction factor is applied to the topography of the valley, then eastern Honey Lake Valley would have an east-sloping gradient.

ACKNOWLEDGMENTS

Funding was provided in part by National Science Foundation grant EAR-9405057, a fellowship from the Mackay School of Mines and U.S. Geological Survey, and a Jonathon O. Davis Scholarship from the Desert Research Institute.

We thank Marty Mifflin, who shared his field notes and wisdom from his shoreline surveys, and Roger Morrison, who also shared his knowledge. Thanks also go to the University of Nevada, Reno, Seismological Laboratory for earthquake data and to the Nevada Bureau of Mines and Geology for digital fault files and the use of Global Positioning Satellite equipment. Ryan Aglietti and Chris Willoughby ably assisted with surveying duties. Discussions with Alan Ramelli, John Caskey, Mark Stirling, John Oswald, Craig dePolo, Fred Nials, Jim Yount, Marith Reheis, Pat Glancy, and the participants of the 1996 Pacific Cell Friends of the Pleistocene field trip helped tremendously. Reviews by John Anderson, Scott Mensing, and Nick Lancaster improved early versions of the manuscript. Additional reviews by Paul Bierman, Thomas Hanks, and Roger Anderson are greatly appreciated. This is Center for Neotectonic Studies Contribution number 32.

REFERENCES CITED

Adams, K. D., 1997, Late Quaternary pluvial history, isostatic rebound, and active faulting in the Lake Lahontan basin, Nevada and California [Ph.D. dissertation]: Reno, University of Nevada, 169 p.

Adams, K. D., and Wesnousky, S. G., 1995, The age and synchroneity of the highest Lake Lahontan shoreline features, northwestern Nevada and northeastern California: Geological Society of America Abstracts with Programs, v. 27, no. 4, p. 32.

Adams, K. D., and Wesnousky, S. G., 1998, Shoreline processes and the age of the Lake Lahontan highstand in the Jessup embayment, Nevada: Geological Society of America Bulletin, v. 110, p. 1318–1332.

Adams, K. D., and Wesnousky, S. G., 1999, The Lake Lahontan highstand: Age, surficial characteristics, soil development, and regional shoreline correlation: Geomorphology (in press).

Anders, M. H., 1994, Constraints on North American plate velocity from the Yellowstone hotspot deformation field: Nature, v. 369, p. 53–55.

Anderson, L. W., and Hawkins, F. F., 1984, Recurrent Holocene strike-slip faulting, Pyramid Lake fault zone, western Nevada: Geology, v. 12, p. 681–684.

Antevs, E., 1925, On the Pleistocene history of the Great Basin, *in* Quaternary climates: Carnegie Institute of Washington Publication 352, p. 51–144.

Bell, J. W., 1984, Quaternary fault map of Nevada, Reno sheet: Nevada Bureau of Mines and Geology Map 79, scale 1:250 000.

Benson, L. V., and Mifflin, M. D., 1986, Reconnaissance bathymetry of basins occupied by Pleistocene Lake Lahontan, Nevada and California: U.S. Geological Survey Water-Resources Investigations Report 85–4262, 14 p.

Benson, L. V., and Peterman, Z., 1995, Carbonate deposition, Pyramid Lake subbasin, Nevada: 3. The use of ^{87}Sr values in carbonate deposits (tufas) to determine the hydrologic

state of paleolake systems: Palaeogeography, Palaeoclimatology, Palaeoecology, v. 119, p. 201–213.
Benson, L. V., and Thompson, R. S., 1987a, Lake-level variation in the Lahontan basin for the past 50 000 years: Quaternary Research, v. 28, p. 69–85.
Benson, L. V., and Thompson, R. S., 1987b, The physical record of lakes in the Great Basin, *in* Ruddiman, W. F., and Wright, H. E., Jr., eds., North America and adjacent oceans during the last deglaciation: Boulder, Colorado, Geological Society of America, Geology of North America, v. K-3, p. 241–260.
Benson, L. V., Meyers, P. A., and Spencer, R. J., 1991, Change in the size of Walker Lake during the past 5000 years: Palaeogeography, Palaeoclimatology, Palaeoecology, v. 81, p. 189–214.
Bills, B. G., and May, G. M., 1987, Lake Bonneville: Constraints on lithospheric thickness and upper mantle viscosity from isostatic warping of Bonneville, Provo and Gilbert stage shorelines: Journal of Geophysical Research, v. 92, p. 11 493–11 508.
Bills, B. G., Currey, D. R., and Marshall, G. A., 1994, Viscosity estimates for the crust and upper mantle from patterns of lacustrine shoreline deformation in the eastern Great Basin: Journal of Geophysical Research, v. 99, p. 22059–22086.
Bills, B. G., Adams, K. D., and Wesnousky, S. G., 1995, Estimates of upper mantle viscosity in the western Great Basin from Lake Lahontan shoreline elevation patterns: Eos (Transactions, American Geophysical Union), v. 76, p. F608.
Bradbury, J. P., Forester, R. M., and Thompson, R. S., 1989, Late Quaternary paleolimnology of Walker Lake, Nevada: Journal of Paleolimnology, v. 1, p. 249–267.
Callaghan, E., and Gianella, V. P., 1935, The earthquake of January 30, 1934, at Excelsior Mountains, Nevada: Seismological Society of America Bulletin, v. 25, p. 161–168.
Caskey, S. J., Wesnousky, S. G., Zhang, P., and Slemmons, D. B., 1996, Surface faulting of the 1954 Fairview Peak (Ms 7.2) and Dixie Valley (Ms 6.8) earthquakes, central Nevada: Seismological Society of America Bulletin, v. 86, p. 761–787.
Cathles, L. M., 1975, The viscosity of the Earth's mantle: Princeton, New Jersey, Princeton University Press, 386 p.
Crittenden, M. D., 1963a, New data on the isostatic deformation of Lake Bonneville: U.S. Geological Survey Professional Paper 454, p. E1–E31.
Crittenden, M. D., 1963b, Effective viscosity of the Earth derived from isostatic loading of Pleistocene Lake Bonneville: Journal of Geophysical Research, v. 68, p. 5517–5530.
Crittenden, M. D., 1967, Viscosity and finite strength of the mantle as determined from water and ice loads: Royal Astronomical Society Geophysical Journal, v. 14, p. 261–279.
Davis, J. O., 1982, Bits and pieces: The last 35 000 years in the Lahontan area, *in* Madsen, D. B., and O'Connell, J. F., eds., Man and environment in the Great Basin: Society of American Archeologists Papers, no. 2, p. 53–75.
Davis, J. O., 1983, Geologic map of the Rye Patch Reservoir South quadrangle, Nevada: Nevada Bureau of Mines and Geology Map 76, scale: 1:24 000.
Davis, J. O., 1987, Geology at Rye Patch, *in* Rusco, M. K., and Davis, J. O., eds., Studies in archeology, geology and paleontology at Rye Patch Reservoir, Pershing County: Nevada State Museum Anthropological Papers, no. 20, p. 9–22.
Davis, J. O., 1990, Giant meanders on Humboldt River near Rye Patch Nevada due to catastrophic flooding: Geological Society of America Abstracts with Programs, v. 22, no. 7, p. A309.
Demsey, K., 1987, Holocene faulting and tectonic geomorphology along the Wassuk Range, west-central Nevada [Master's thesis]: Tucson, University of Arizona, 64 p.
Dixon, T. H., 1991, An introduction to the global positioning system and some geological applications: Reviews of Geophysics, v. 29, p. 249–276.
Dodge, R. L., 1982, Seismic and geomorphic history of the Black Rock fault zone, northwest Nevada [Ph.D. dissertation]: Golden, Colorado School of Mines, 213 p.
Dohrenwend, J. C., Schell, B. A., Menges, C. M., Moring, B. C., and McKittrick, M. A., 1996, Reconnaissance photogeologic map of young (Quaternary and late Tertiary) faults in Nevada, *in* Singer, D. A., ed., An analysis of Nevada's metal-bearing mineral resources: Nevada Bureau of Mines and Geology Open-File Report 96-2, 167 p., scale 1: 1 000 000.
Duffy, W., Belknap, D. F., and Kelley, J. T., 1989, Morphology and stratigraphy of small barrier-lagoon systems in Maine: Marine Geology, v. 88, p. 243–262.
Gianella, V. P., 1957, Earthquake and faulting, Fort Sage Mountains, California, December, 1950: Seismological Society of America Bulletin, v. 47, p. 173–177.
Gianella, V. P., and Callaghan, E., 1934a, The earthquake of December 20, 1932, at Cedar Mountain, Nevada, and its bearing on the genesis of Basin-Range structure: Journal of Geology, v. 42, p. 1–22.
Gianella, V. P., and Callaghan, E., 1934b, The Cedar Mountains, Nevada, earthquake of December 20, 1932: Seismological Society of America Bulletin, v. 24, p. 345–384.
Gilbert, G. K., 1890, Lake Bonneville: U.S. Geological Survey Monograph 1, 438 p.
Grose, T. L. T., Saucedo, G. J., and Wagner, D. L., 1990, Geologic map of the Susanville quadrangle, Lassen and Plumas Counties, California: California Department of Conservation Division of Mines and Geology Open-File Report 91-1, 26 p., scale 1: 1 000 000.
Hanks, T. C., and Wallace, R. E., 1985, Morphological analysis of the Lake Lahontan shoreline and beach front fault scarps, Pershing County, Nevada: Seismological Society of America Bulletin, v. 75, p. 835–846.
Hawley, J. W., and Wilson, W. E., 1965, Quaternary geology of the Winnemucca area, Nevada: Reno, Nevada, Desert Research Institute Technical Report no. 5, 66 p.
Humphreys, E. D., and Dueker, K. G., 1994a, Western U.S. upper mantle structure: Journal of Geophysical Research, v. 99, p. 9615–9634.
Humphreys, E. D., and Dueker, K. G., 1994b, Physical state of the western U.S. upper mantle: Journal of Geophysical Research, v. 99, p. 9635–9650.
Jones, J. C., 1925, The geologic history of Lake Lahontan, *in* Quaternary climates: Carnegie Institute of Washington Publication 35, p. 1–50.
Jones, J. C., 1933, Itinerary, Reno to Pyramid Lake and return, *in* Jenkins, O. P., ed., Middle California and western Nevada (Excursion C-1): International Geological Congress, XVI session, Washington, D.C., Guidebook 16, p. 102–108.
King, C. A. M., 1972, Beaches and coasts (second edition): London, Edward Arnold, 570 p.
King, G. Q., 1978, The Quaternary history of Adrian Valley, Lyon County, Nevada [Master's thesis]: Salt Lake City, University of Utah, 88 p.
King, G. Q., 1993, Late Quaternary history of the lower Walker River and its implications for the Lahontan paleolake system: Physical Geography, v. 14, p. 81–96.
Lachenbruch, A. H., 1978, Heat flow in the Basin and Range province and thermal effects of tectonic extension: Pure and Applied Geophysics, v. 117, p. 34–50.
McKee, E. H., and Noble, D. C., 1986, Tectonic and magmatic development of the Great Basin of western United States during late Cenozoic time: Modern Geology, v. 10, p. 39–49.
McQuarrie, N., and Rodgers, D. W., 1998, Subsidence of a volcanic basin by flexure and lower crustal flow: The eastern Snake River Plain, Idaho: Tectonics, v. 17, p. 203–220.
Mifflin, M. D., 1984, Paleohydrology of the Lahontan basin, *in* Lintz, J., ed., Western geological excursions, Volume 3: Reno, Nevada, Mackay School of Mines, p. 134–137.
Mifflin, M. D., and Wheat, M. M., 1971, Isostatic rebound in the Lahontan basin, northwestern Great Basin: Geological Society of America Abstracts with Programs, v. 3, p. 647.
Mifflin, M. D., and Wheat, M. M., 1979, Pluvial lakes and estimated pluvial climates of Nevada: Nevada Bureau of Mines and Geology Bulletin 94, 57 p.
Minster, J. B., and Jordan, T. H., 1987, Vector constraints on western U.S. deformation from space geodesy, neotectonics and plate motions: Journal of Geophysical Research, v. 92, p. 4798–4804.
Morgan, P., and Gosnold, W. D., 1989, Heat flow and thermal regimes in the continental United States, *in* Pakiser, L. C., and Mooney, W. D., eds., Geophysical framework of the continental United States: Geological Society of America Memoir 172, p. 493–522.
Morrison, R. B., 1991, Quaternary stratigraphic, hydrologic, and climatic history of the Great Basin, with emphasis on Lakes Lahontan, Bonneville, and Tecopa, *in* Morrison, R. B., ed., Quaternary nonglacial geology: Conterminous U.S.: Boulder, Colorado, Geological Society of America, Geology of North America, v. K-2, p. 283–320.
Morrison, R. B., and Davis, J. O., 1984, Quaternary stratigraphy and archeology of the Lake Lahontan area; a re-assessment, *in* Lintz, J., ed., Western geological excursions, Volume 1: Reno, Nevada, Mackay School of Mines, p. 252–281.
Morrison, R. B., Mifflin, M. D., and Wheat, M., 1965, Badland amphitheater on the Truckee River north of Wadsworth, *in* Wahrhaftig, C., Morrison, R. B., and Birkeland, P. W., eds., Guidebook for Field Conference I, Northern Great Basin and California: International Association for Quaternary Research, 7th Congress: Lincoln, Nebraska Academy of Science, p. 38–43.
Nakiboglu, S. M., and Lambeck, K., 1982, A study of the Earth's response to surface loading with applications to Lake Bonneville: Royal Astronomical Society Geophysical Journal, v. 70, p. 577–620.
Nakiboglu, S. M., and Lambeck, K., 1983, A reevaluation of the isostatic rebound of Lake Bonneville: Journal of Geophysical Research, v. 88, p. 10 439–10 447.
Oppliger, G. L., Murphy, J. B., and Brimhall, G. H., 1997, Is the ancestral Yellowstone hotspot responsible for the Tertiary "Carlin" mineralization in the Great Basin of Nevada?: Geology, v. 25, p. 627–630.
Parsons, T., Thompson, G. A., and Smith, R. P., 1998, More than one way to stretch: A tectonic model for extension along the plume track of the Yellowstone hotspot and adjacent Basin and Range Province: Tectonics, v. 17, p. 221–234.
Passey, Q. R., 1981, Upper mantle viscosity derived from the difference in rebound of the Provo and Bonneville shorelines: Lake Bonneville Basin: Journal of Geophysical Research, v. 86, p. 11 701–11 708.
Peltier, W. R., 1986, Deglaciation-induced vertical motion of the North American continent and transient lower mantle rheology: Journal of Geophysical Research, v. 91, no. B9, p. 9099–9123.
Reheis, M. C., 1996, Old, very high pluvial lake levels in the Lahontan basin, Nevada: Evidence from the Walker Lake basin, *in* Adams, K. D., and Fontaine, S. A., eds., Quaternary history, isostatic rebound and active faulting in the Lake Lahontan basin, Nevada and California: Reno, Nevada, Pacific Cell Friends of the Pleistocene Field Trip Guidebook, p. 99–118.
Rockwell, G. L., 1990, Surface-water hydrology of Honey Lake Valley, Lassen County, California, and Washoe County, Nevada: U.S. Geological Survey Open-File Report 90-177, 2 sheets.
Rogers, A. M., Harmsen, S. C., Corbett, E. J., Priestley, K., and dePolo, D., 1991, The seismicity of Nevada and some adjacent parts of the Great Basin, *in* Slemmons, D. B., Engdahl, E. R., Zoback, M. D., and Blackwell, D. D., eds., Neotectonics of North America: Boulder, Colorado, Geological Society of America, Geology of North America, Decade Map Volume, p. 153–184.
Russell, I. C., 1885, Geological history of Lake Lahontan, a Quaternary lake in northwestern Nevada: U.S. Geological Survey Monograph 11, 288 p.
Sanders, C. O., and Slemmons, D. B., 1979, Recent crustal movements in the central Sierra Nevada–Walker Lane region of California-Nevada: Part III, The Olinghouse fault zone: Tectonophysics, v. 52, p. 585–597.
Slemmons, D. B., 1957a, Geologic setting for the Fallon-Stillwater earthquakes of 1954: Seismological Society of America Bulletin, v. 47, p. 4–9.
Slemmons, D. B., 1957b, Geological effects of the Dixie Valley–Fairview Peaks, Nevada, earthquakes of December 16, 1954: Seismological Society of America Bulletin, v. 47, p. 353–375.
Smith, G. I., and Street-Perrott, F. A., 1983, Pluvial lakes of the western United States, *in* Porter, S. C., ed., The late Pleistocene: Minneapolis, University of Minnesota Press, p. 190–211.
Smith, R. B., and Braile, L. W., 1994, The Yellowstone hotspot: Journal of Volcanology and Geothermal Research, v. 61, p. 121–187.
Smoot, J. P., 1993, Field trip guide: Quaternary-Holocene lacustrine sediments of Lake Lahontan, Truckee River Canyon north of Wadsworth, Nevada: U.S. Geological

Survey Open-File Report 93–689, 35 p.
Sokkisha Co., LTD, 1991, Sokkia Set 2B Electronic Total Station operators manual: Tokyo, Japan, 84 p.
Stewart, J. H., 1978, Basin and Range structure in western North America, A review, *in* Smith, R. B., and Eaton, G. P., eds., Cenozoic tectonics and regional geophysics of the Western Cordillera: Geological Society of America Memoir 152, p. 1–32.
Stewart, J. H., 1988, Tectonics of the Walker Lane belt, western Great Basin: Mesozoic and Cenozoic deformation in a zone of shear, *in* Ernst, W. G., ed., Metamorphism and cause of evolution of the western United States: Ruby Volume 7: Englewood Cliffs, New Jersey, Prentice-Hall, p. 683–713.
Stine, S. W., 1994, Droughts and deluges in late Holocene California: The record from lake fluctuations and drowned stumps: Eos (Transactions, American Geophysical Union), v. 75, p. 370.
Strahler, A. H., and Strahler, A. N., 1992, Modern physical geography (fourth edition): New York, John Wiley and Sons, 638 p.
Thatcher, W., Foulger, G. R., Julian, B., Svarc, J., Quilty, E., and Bawden, G. W., 1999, Present-day deformation across the Basin and Range province, western United States: Science, v. 283, p. 1714–1718.
Thompson, G. A., Catchings, R., Goodwin, E., Holbrook, S., Jarchow, C., Mann, C., McCarthy, J., and Okaya, D., 1989, Geophysics of the western Basin and Range province, *in* Pakiser, L. C., and Mooney, W. D., eds., Geophysical framework of the continental United States: Geological Society of America Memoir 172, p. 177–203.
Thompson, R. S., Benson, L. V., and Hattori, E. M., 1986, A revised chronology for the last Pleistocene lake cycle in the central Lahontan basin: Quaternary Research, v. 25, p. 1–9.
VanWormer, J. D., and Ryall, A. S., 1980, Sierra Nevada–Great Basin boundary zone: Earthquake hazard related to structure, active tectonic processes, and anomalous patterns of earthquake occurrence: Seismological Society of America Bulletin, v. 70, p. 1557–1572.
Walcott, R .I., 1970, Flexural rigidity, thickness and viscosity of the lithosphere: Journal of Geophysical Research, v. 75, p. 3941–3954.
Wallace, R. E., 1984a, Patterns and timing of late Quaternary faulting in the Great Basin Province and relation to some regional tectonic features: Journal of Geophysical Research, v. 89, p. 5763–5769.
Wallace, R. E., 1984b, Fault scarps formed during the earthquakes of October 2, 1915, in Pleasant Valley, Nevada, and some tectonic implications in faulting related to the 1915 earthquakes in Pleasant Valley, Nevada: U.S. Geological Survey Professional Paper 1274-A, 33 p.
Wallace, R. E., 1987, Grouping and migration of surface faulting and variations in slip rates on faults in the Great Basin Province: Seismological Society of America Bulletin, v. 77, p. 868–876.
Weick, R. J., 1990, Structural, tectonic and Quaternary study of the eastern Madeline Plains, California and southwestern Smoke Creek Desert, Nevada [Master's thesis]: Reno, University of Nevada, 160 p.
Wills, C. J., and Borchardt, G., 1993, Holocene slip rate and earthquake recurrence on the Honey Lake fault zone, northeastern California: Geology, v. 21, p. 853–856.
Zoback, M. L., 1989, State of stress and modern deformation of the northern Basin and Range province: Journal of Geophysical Research, v. 94, p. 7105–7128.

MANUSCRIPT RECEIVED BY THE SOCIETY JULY 6, 1998
MANUSCRIPT ACCEPTED DECEMBER 17, 1998

Printed in U.S.A.